



Step-drawdown test as a tool for the assessment of the Nubia sandstone aquifer in East El-Oweinat Area, Egypt

Bassem S. Nabawy¹ · Ahmed Abdelhalim² · Ahmed El-Meselhy¹

Received: 10 October 2018 / Accepted: 17 June 2019 / Published online: 25 June 2019
© Springer-Verlag GmbH Germany, part of Springer Nature 2019

Abstract

The Cretaceous Nubia sandstone aquifer is the main aquifer in East El-Oweinat area along the Egyptian–Sudanese borders and in NE Africa. East El-Oweinat project has been recently considered one of the main agricultural projects in the southwest of the Egyptian Western Desert. So, the hydrogeological assessment for the Nubia aquifer in East El-Oweinat area has been done through studying and characterising the hydraulic parameters and step-drawdown test. The well and aquifer losses coefficients (C and B , respectively), the specific capacity, and the well efficiency as well as the aquifer and aquitard thickness have been estimated and traced through a total of 46 wells that have been distributed through the study area in two sectors, southern and northern. For the purpose of further exploration, the effective porosity (\emptyset), hydraulic conductivity (K), and transmissivity (T) have been estimated for the wells in the northern sector. In addition, an aquifer assessment quality index has been introduced to assess and to rank the studied aquifer. Therefore, it is concluded that the hydraulic and the step-drawdown parameters as well as the aquifer and aquitard thicknesses are prospective for further exploration to the north and the east of the northern sector in the study area. The well efficiency is mostly affected by the studied parameters, particularly the well loss coefficient, the hydraulic parameters and the well design as well. GIS approach and ArcGIS software have been applied to delineate the spatial distribution of the well performance characteristics, in order to compare between the studied groundwater wells and to integrate the different-acquired data. A set of isocontour maps have been introduced to match the lateral variation of the studied parameters and the aquifer potential to refer to the best direction for further underground water exploration.

Keywords East El-Oweinat · Transmissivity · Hydraulic conductivity · Aquifer losses · Well efficiency · GIS system

Introduction

East El-Oweinat project, to the East of Gebel El-Oweinat, is one of the most important development agricultural projects in Egypt. It is located at the far southwestern part of Western Desert of Egypt (Fig. 1). The area is bounded by Dakhla and Kharga Oases to the north, the Egyptian-Sudanese borders to the south, Lake Nasser and Toshka Lakes to the east, as well as Gebel El-Oweinat and El-Gilf El-Kebir plateau to the west. The study area is located between latitudes 22°41'12"N

and 22°51'12", and longitudes 28°24'12" and 28°34'12"E, covering an area of 384 km² (about 94,888 feddans, Fig. 1).

The Nubia sandstone is among the highly porous and permeable rock sequences in Egypt and is considered the main strategic producing aquifers in North Africa. Its age and classification are a matter of controversy due to its bareness of fossils and similarity in the mineral composition (Nabawy et al. 2009, 2010; Nabawy and Géraud 2016). It has been studied in its type sections by many workers, e.g. Said (1962), Issawi (1973), Klitzsch (1979, 1984), Issawi and Jux (1982), Hendriks (1988), Issawi and Osman (1993), Thabit (1994), Nabawy et al. (2009, 2010), etc. In general, it is composed of Cretaceous varicolored fine- to medium-grained sandstone intercalated with some water-baffle to barrier beds (aquitard) of clays, shale and siltstones. These rock sequences have suffered from a long arid periods which increased their final porosity and permeability. Therefore, their storage and flow capacity have

✉ Bassem S. Nabawy
bsnabawy@yahoo.co.uk

¹ Department of Geophysical Sciences, National Research Centre, Cairo, Egypt

² Geology Department, Faculty of Science, Cairo University, Giza, Egypt

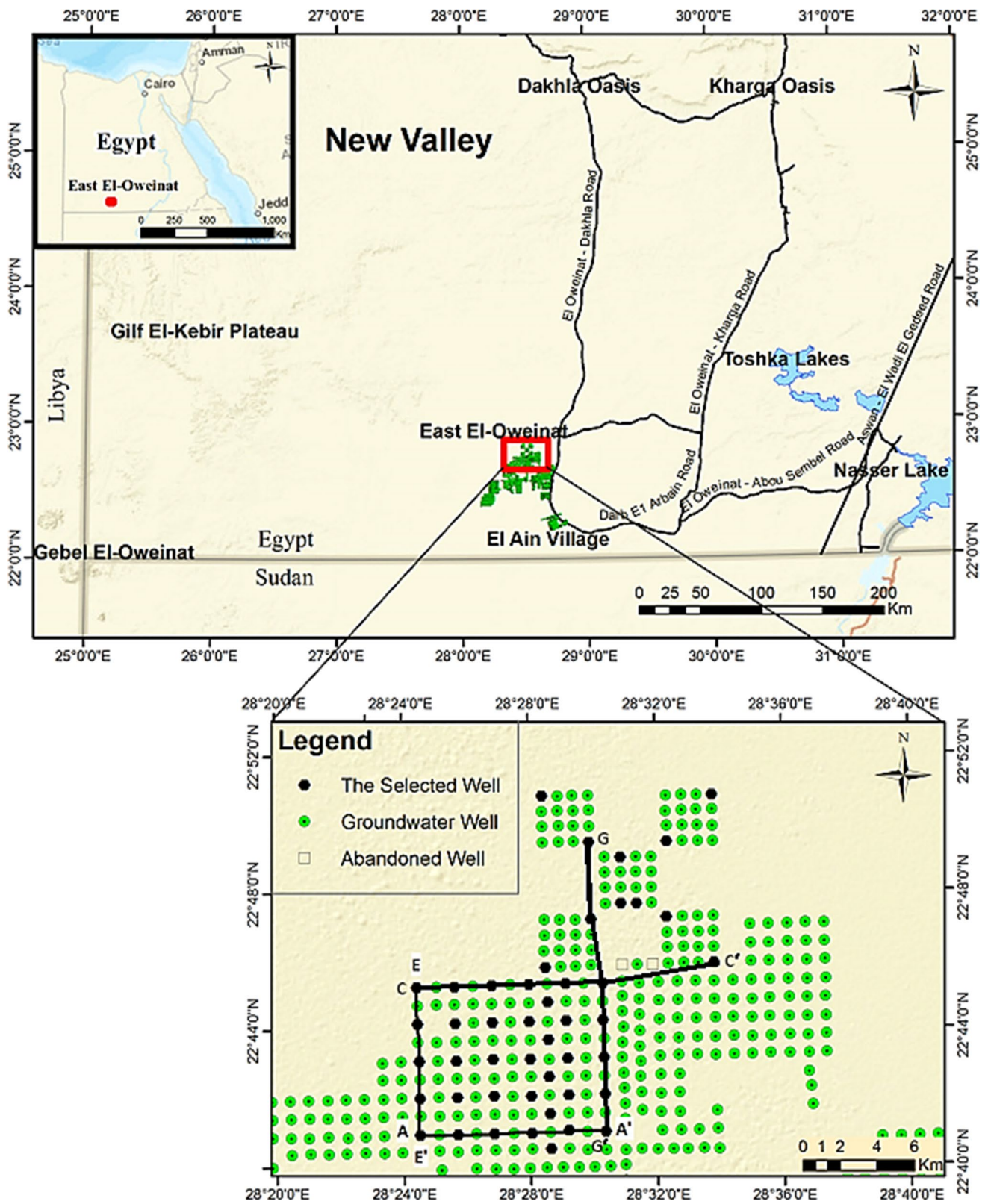


Fig. 1 Location map for the study area in East El-Oweinat, SW Egypt. The location of the studied subsurface cross sections are also indicated, E-E', G-G', C-C' and A-A'

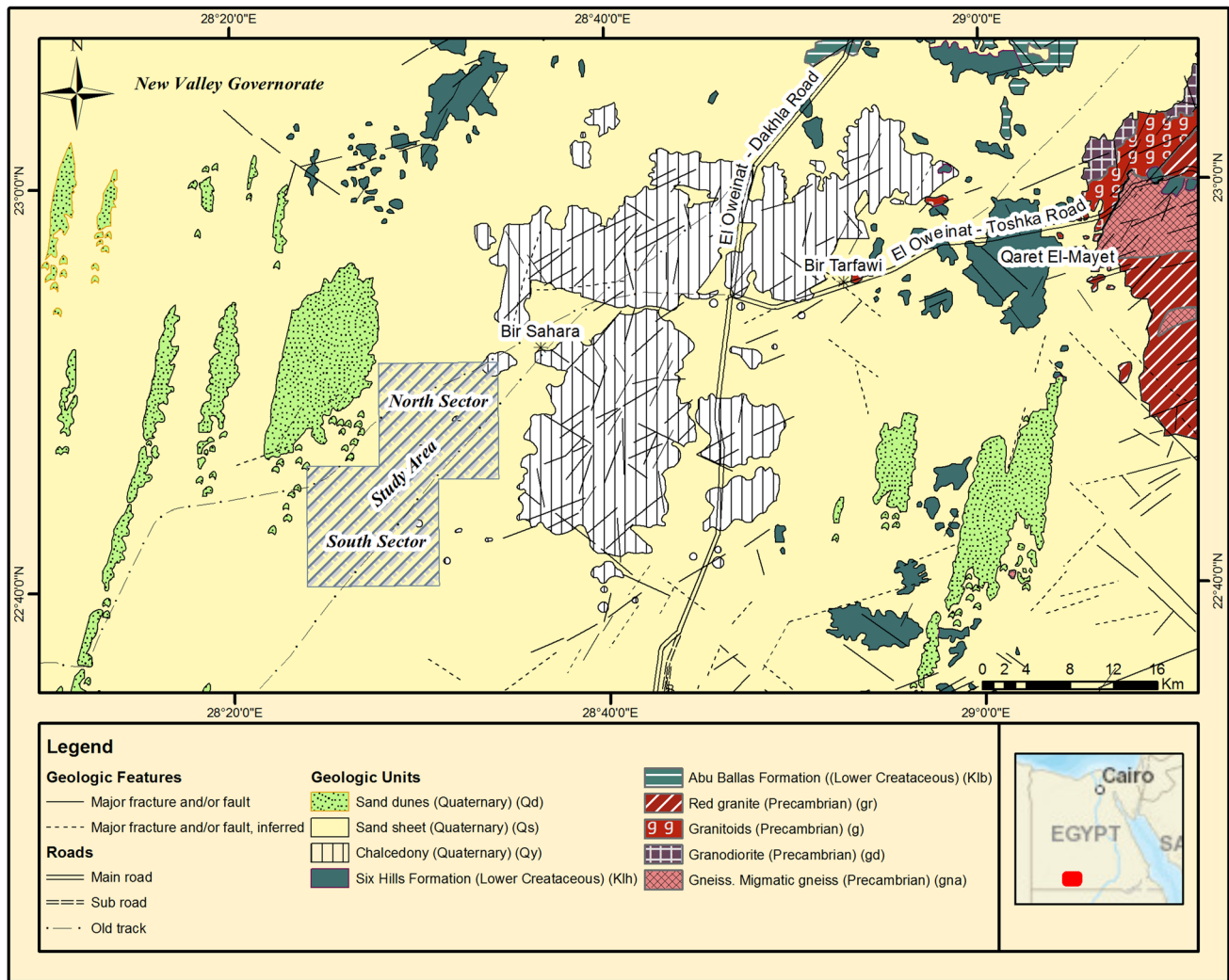


Fig. 2 Geological map of East El-Oweinat area in SW Egypt showing the study area (redrawn after CONOCO, 1987)

been increased to serve as potential aquifers and reservoirs in different localities (Nabawy et al. 2009, 2010).

To achieve the best understanding for the aquifer behaviour and production, it is important to measure and calculate its hydraulic parameters including the hydraulic conductivity, transmissivity, and aquifer assessment index as well as the aquifer and aquitard thickness.

Step-drawdown test is accomplished for a total of 46 groundwater wells in East El-Oweinat area. It is a procedure based on some pressure-built up and drawdown consequent steps, applied to determine the hydraulic parameters and the well performance characteristics, such as the well and aquifer losses, specific capacity, well efficiency and optimum pumping rates. In addition, integration of the obtained hydrogeological data into GIS system has been developed as a mean for assembling and analysing diverse spatial data. Hence, different thematic maps have

been constructed for the different hydrogeological parameters for the aquifer system in the studied area.

Geologic setting

The main geologic units in East El-Oweinat are described by many authors such as Klitzsch (1984), Thabit (1994), and Nabawy et al. (2009, 2010), etc. The oldest rocks in the East El-Oweinat area are the Precambrian basement rocks which are described as Aswan red/rose granites, granodiorite and granitoids associated with some basic gneiss, migmatic gneiss, some amphibolite, calc-silicate rocks and marbles intersected with some basalt dykes and sills intersecting the different rock sequences. The basement is unconformably overlain by a dominating sandy section belonging to the Upper Cretaceous Nubia sandstone which was classified into the Six Hills Formation and Abu Ballas Formation (Fig. 2).

The Six Hills Formation has a maximum thickness attains 500 m at its type section near the Six Hills village. It is composed of medium- to coarse-grained sandstone, having different colours and its texture ranges from friable to highly consolidated cross-bedded sandstones. It is summed up into fining upward cycles starting at the base with erosional surface followed upward with tabular cross-bedded sandstones (good storage units), kaolinitic sandstones and topped with paleosols with much plant roots (aquitards) with burrowing activities at the top of each cycle. To the east of the studied area, the depositional cycles were always topped by thin oolitic ironstone beds (5–15 cm). The arid weather (that prevailed for long geological periods), fracturing, dissolution and leaching out of some of the ironstone beds resulted in the presence of some vertical and inclined laminas filling the dominant fractures. The Six Hills Formation is equivalent to Adindan and Abu Simbil Formations in Tushka area (Nabawy and Géraud 2016).

Upwards, the Abu Ballas Formation has a thickness ranging from few metres up to 100 m at its type section near Abu Ballas Village (Fig. 2). It is equivalent to the Lingula Shale of Klitzsch (1979). Its lower parts are composed of cross-bedded, reddish yellow, highly fractured and block sandstones, pebbly upwards, and interbedded with greyish coloured shales. Upwards, it is composed of yellowish white cross-bedded, coarse grained and pebbly sandstones intercalated and topped with thin beds of oolitic ironstone (5–15 cm).

The Nubia sandstone aquifer system ‘NSAS’ is the main groundwater aquifer in East El-Oweinat area. Its sequence is not differentiated in the subsurface of the study area, but based on the field relationships it is thought to be composed mostly of the Six Hills Formation. The hydrological and the hydrogeological of the ‘NSAS’ have been studied in many productive and observatory wells drilled by the General Petroleum Company ‘GPC’ (Nour 1979; GPC 1984; Nour 1996). The underground water of the Nubia aquifer seems to be fossil water trapped in the past periods through surface water infiltration during the rainy periods (Thorweihe and Heintz 1993). In East El-Oweinat area, the Nubia sequence has been dominated by a long history of tectonism and prevailing arid weather which increased the fracture porosity and hydraulic conductivity of the Nubia sandstone (Nabawy and Géraud 2016). Sometimes, the Nubia sandstone is intensively ferruginated and/or silicified, forming hard and compacted quartzite rocks due to the metamorphism of the sandstone, e.g. at Qaret El-Mayet (Fig. 2).

It is followed upward by Quaternary deposits in East El-Oweinat area. These widespread Quaternary deposits are represented by chalcidony, lake deposits/playa and eolian deposits as sand dunes and sheets. The sand dunes are aligned toward NE–SW direction, forming either continuous belts or isolated crescent-shaped sand dunes (Fig. 2). The

chalcidony sheets cover most of the area surrounding the study area with thickness reaches up to 30 m of milky, earthy and white colours, forming hummocky cross-stratification surface.

Materials and methods

The step-drawdown test has been carried out for each of 46 groundwater wells in the study area of East El-Oweinat. The studied wells are equally distributed in two square sectors: northern (11 wells) and southern sectors (36 wells) (Fig. 1). This is carried out to determine the well performance characteristics. The step-drawdown pumping test has been performed in a single pumping well to investigate the performance of a pumping well under controlled variable discharge conditions without serving additional observation wells, i.e. it is applied in each well separately. In the test, the discharge rate is investigated in the step-drawdown well by increasing the discharge rate and the water level within the same well was recorded and the drawdown for each rate was determined. The entire test takes place over the course of 1 day, using at least three pumping steps of equal duration, lasting 120 min for each step to allow dissipation of wellbore storage effects (Kruseman and de Ridder 1994, 2000). As an example, procedure and results of the three steps of the step-drawdown test for the groundwater well (A5) in the study area are presented in Fig. 3a and summarised in Table 1.

The behaviour of the groundwater well can be summarised by a relationship expressing the drawdown ‘ S ’, in m, in a pumping well as a function of the discharge rate ‘ Q ’, in m^3/h . Therefore, Jacob (1947) first proposed the following relationship:

$$S = BQ + CQ^2, \quad (1)$$

where B is the aquifer loss coefficient (h/m^2), and C is the well loss coefficient (h^2/m^5).

A number of methods have been developed for determining the B and C coefficients. One of the simplest and most common methods is called “Hantush-Bierschenk method”, which is compiled by many authors such as Jacob (1950), Bruin and Hudson (1955), Bierschenk and Wilson (1961), Kawecki (1995), and Kruseman and de Ridder (2000).

The Hantush-Bierschenk method is a straight-line step-drawdown test analysis for graphical plot of the specific drawdown ‘ S/Q ’ as a function of discharge ‘ Q ’ for estimating the aquifer and well losses coefficients, B and C , respectively. As an example, plotting the specific drawdown ‘ S/Q ’ as a function of the pumping rate ‘ Q ’ indicates a straight line (Fig. 3b). The intercept of this line with y-axis equals the formation aquifer loss coefficient ‘ B ’ and the slope of this line equals the well loss coefficient (C) (Bierschenk 1963; Hantush 1964).

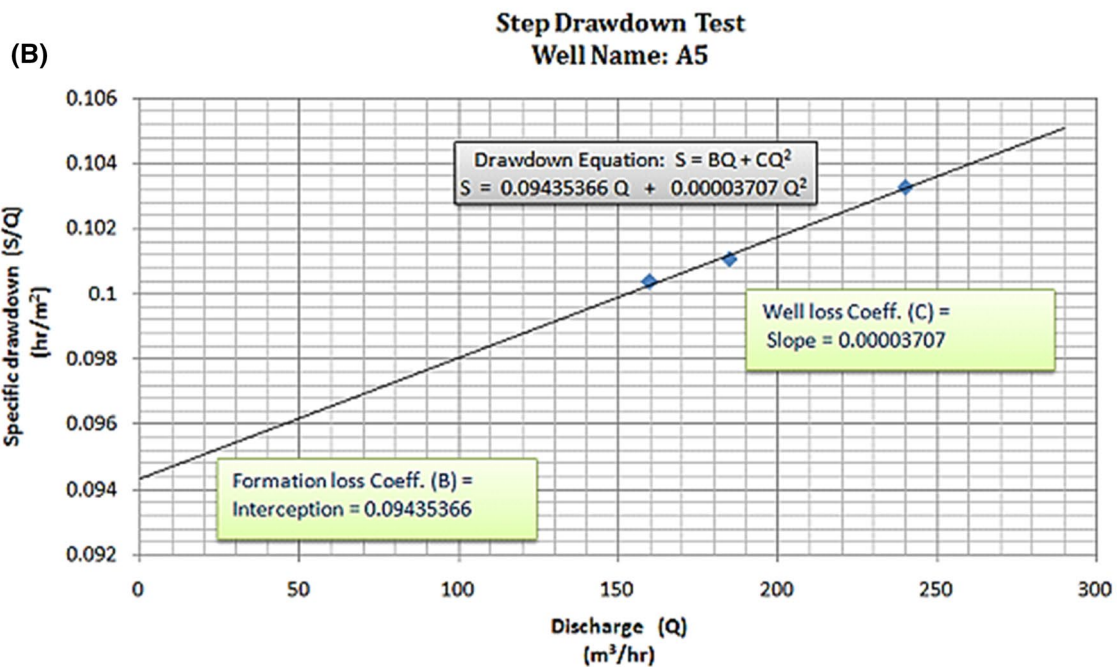
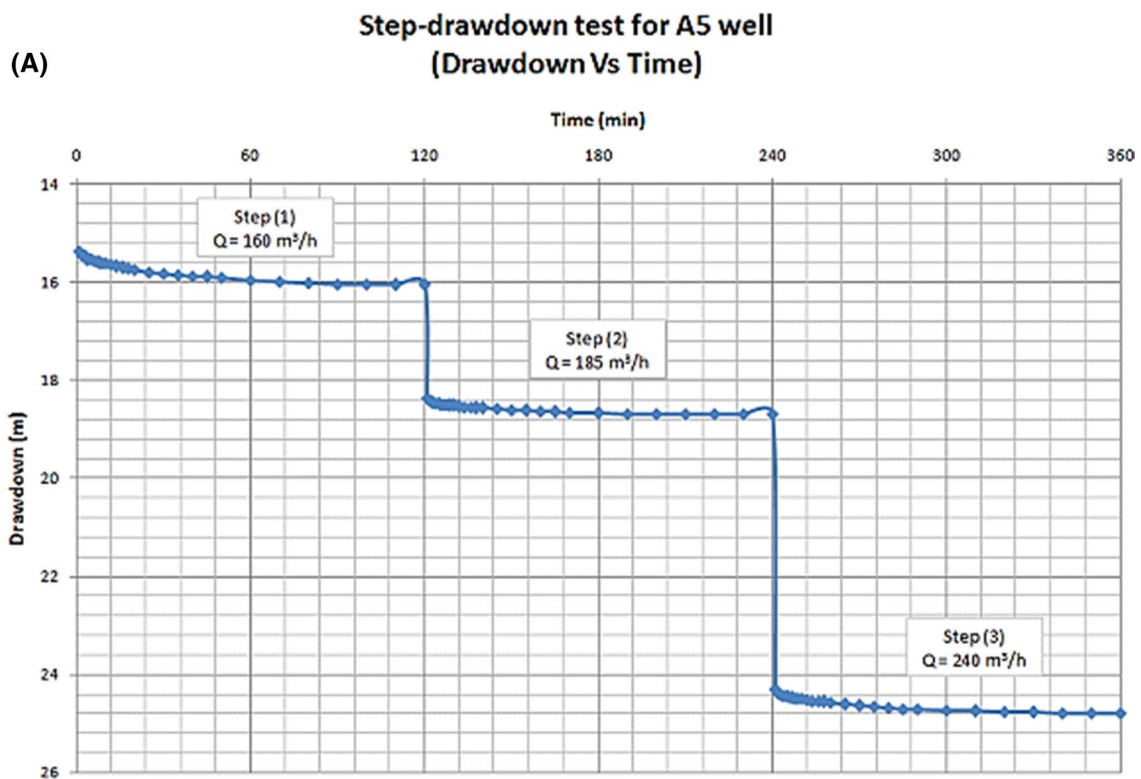


Fig. 3 a Sketch showing the step-drawdown test represented by the drawdown as a function of time through three steps, each lasted for 2 h, and **b** determination of the coefficients of aquifer and well losses

(**b, c, respectively**) using the a graphical presentation for the step-drawdown test, example from A5 well, East El-Oweinat area

Table 1 Results of the three steps of the drawdown test in A5 well in the study area

Real data of the drawdown test			Calculated data	
Step drawdown test no.	Discharge (Q) (m ³ /h)	Max. drawdown (m)	Specific drawdown (S/Q) (h/m ²)	Well efficiency (%)
Step test no. (1)	160	16.06	0.10037500	94.09
Step Test No. (2)	185	18.70	0.10108108	93.22
Step test no. (3)	240	24.79	0.10329167	91.40

The well efficiency of the pumped well is then calculated as the ratio of the aquifer loss to the total head loss (Mogg 1969; Todd 1980). It represents the relationship between the calculated theoretical drawdown outside the well and the measured drawdown inside the well (Kruseman and de Ridder 1994, 2000). It can be determined by the following:

$$\text{Well efficiency (\%)} = \frac{BQ}{BQ + CQ^2} \times 100, \quad (2)$$

where BQ is the aquifer loss, CQ^2 is the turbulent head loss and $(BQ + CQ^2)$ is the total head loss.

As the pumping rate Q increases, the drawdown increases; hence the well efficiency decreases. The well efficiency ' W_{eff} ' and specific capacity ' Sc ' have been calculated at a discharge rate ' Q ' equals 250 m³/h as a safe yield (recommended by RIGW 2008).

The specific capacity ' Sc ' (equals to Q/S , i.e. it is the reciprocal of the specific drawdown) is identified as "the quantity of groundwater produced in a well per unit of drawdown". It decreases with increasing the pumping rate ' Q '. It is a derivation of Eq. (1), where the specific capacity (in m²/h) for each well can be calculated as follows:

$$\text{Specific capacity 'Sc'} = \frac{Q}{S} = \frac{1}{B + CQ} \quad (3)$$

For the present study, the effective porosity \emptyset_{eff} is calculated using the available R16 and R64 well log data for the studied wells in the northern sector of the study. \emptyset_{eff} is a function of both the true resistivity (Rt) of the studied aquifer and resistivity of its water content (Rw). Based on the chemical analysis of the groundwater in the intensive study area, the water type is "Sodium Chloride, NaCl"; therefore, the following equation has been applied to determine effective porosity (Guyod 1966):

$$\emptyset_{\text{eff}} = \left(\frac{Rw \times 5400}{Rt} \right)^{\frac{1}{2}} \text{ for NaCl water type} \quad (4)$$

The aquifer water resistivity ' Rw ' has been determined from its reciprocal equivalent value, the electrical conductance ' EC ' of the collected groundwater samples.

Transmissivity (T , in m²/day) is defined as the rate of flow under a hydraulic pressure gradient equal to unity through a cross-section of a unit width over the whole saturated thickness

of an aquifer. Therefore, it is a function of the flowing liquid and the petrophysical properties of the aquifer as well as the saturated thickness (H). It is the product of the hydraulic conductivity (K , in m/day) and the saturated thickness ' H ' (in m) of the unconfined aquifer, whereas ' H ' for the confined aquifers is average of height of pressure head of two wells. Therefore, for the present unconfined aquifer transmissivity can be estimated using the following equation:

$$T = K \times H \quad (5)$$

Moreover, the hydraulic conductivity ' K ' and transmissivity ' T ' were calculated for each well in the northern sector (11 wells) for the purpose of further exploration to the north and east. The hydraulic conductivity ' K ' is a measure of the rate at which groundwater can be transmitted through a unit cross-sectional area of the aquifer under a hydraulic pressure gradient of unity. It is used to describe the ease at which water can move through pore spaces of the saturated zones. It is a function of the pore fabric including porosity, viscosity of the flowing fluid, the irreducible water saturation as well as the tortuosity and diameter of pore channels through which the fluid is flowing (Nabawy 2014, 2015; Nabawy et al. 2015). For the intensive study area, the hydraulic conductivity ' K ' (in cm/s) was determined as a function of porosity ' \emptyset_{eff} ' (in decimal) by applying the Marotz's Equation (1968) as follows:

$$\emptyset_{\text{eff}} = 0.462 + 0.045 \text{ Ln } K \quad (6)$$

To assess and to rank the studied Nubia aquifer through the different wells, a new parameter, called aquifer assessment index (AAI), has been proposed in the field of hydrogeology, similar to the reservoir quality index of Amaefule et al. (1993) which has been tested for long decades in the field of petroleum geology. For the present study and for the field of hydrogeological it can be calculated using the available hydraulic conductivity, in m/s, by estimating the permeability in μm^2 . The AAI parameter can be calculated from the hydraulic conductivity as follows:

$$\text{AAI} = \sqrt{\frac{k}{\emptyset}} = \sqrt{\frac{K \cdot \mu}{\rho \cdot g \cdot \emptyset}}, \quad (7)$$

where AAI is the aquifer assessment index in μm , k is the aquifer permeability in μm^2 , \emptyset is porosity in decimals, K is the hydraulic conductivity in cm/s, μ is the water viscosity

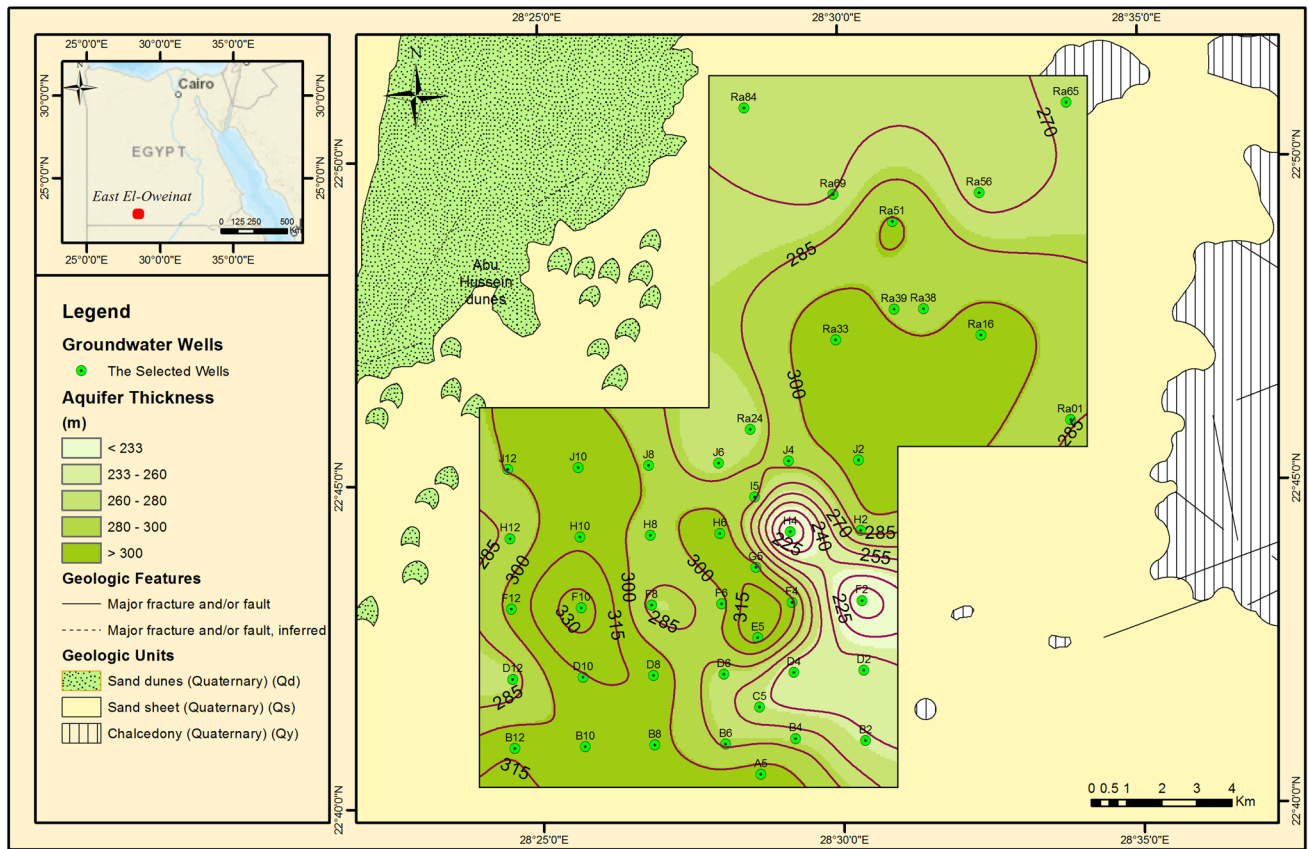


Fig. 4 Isocontour map showing the aquifer thickness in the study area, East El-Oweinat

($=0.01792 \text{ g}/(\text{cm}\cdot\text{s})$), ρ is the water density in g/cm^3 , and g is the earth’s gravity acceleration ($=980 \text{ cm}/\text{s}^2$).

Finally, geographic information system (GIS) approach has been applied to delineate the spatial distribution of the well performance characteristics, in order to compare between the studied groundwater wells and integrate the different-acquired data. The Using of ArcGIS software for multi-layering mapping offers the ability to store, manipulate and analyse data in different formats and at different scales.

Results

Hydrogeological regime

Based on the well log data and the lithology description of the obtained cutting samples during drilling of the studied wells, the aquifer thickness in the southern sector of the study area increases from 195.6 and 200.4 m (at H4 and F2 wells, respectively) in the SE of the study area to 336.8 m (at F10 well) in the SW of the study area, of average 287.7 m (Fig. 4, Table 2). The aquifer thickness in the northern sector indicates a high aquifer potential; it reaches up to 286.4 m (at Ra01 well) in the SE, 273.0 m

(at Ra65 well) in the NE, and 266.7 m (at Ra84 well) in the NW of the northern sector with average thickness equal to 286.0 m which is similar to the southern sector (Fig. 4, Table 2). In general, the aquifer thickness slightly decreases toward the northern sector, around Ra56 and Ra69 wells. The thickness is also dramatically decreased toward the southeastern direction, around H4, F2 and B2 wells, due to the decrease of the total thickness of the Nubia sandstone.

Studying effects of increasing the aquifer thickness and decreasing the aquitard thickness helps in estimating the potential of the studied Nubia sandstone as a strategic aquifer in Ease El-Oweinat area. For the present study, the aquitard thickness in the studied wells varies from 83.3 m (at Ra84 well), 77.0 m (at Ra65 well) to the NW and NE, respectively, of the northern sector of the studied area, and 85.1 m (at H8 well) to the centre of the southern sector of the study area, to 10.8 m (at H4 well) and 13.6 m (at F10 well) in the centre of the southern sector of the study area (Fig. 5, Table 2). The average aquitard thickness in the southern sector equals about 47.5 m while increases in the northern sector to 58.8 m. However, the aquitard thickness increases with decreasing net aquifer thickness.

Table 2 The hydraulic parameters of the studied wells including aquifer thickness, aquitard thickness, the well loss coefficient (C), aquifer loss coefficient (B), specific capacity (Sc) and well efficiency (W_{eff}) for the studied wells in East El-Oweinat area, SW Egypt

S no.	Well no.	Aquifer Th. (m)	Aquitard Th. (m)	C h^2/m^5	B h/m^2	Sc m^2/h	W_{eff} %	S no.	Well no.	Aquifer Th. (m)	Aquitard Th. (m)	C h^2/m^5	B h/m^2	Sc m^2/h	W_{eff} %
1	Ra01	286.4	63.6	0.0000466	0.0362608	20.87	75.69	24	D10	313.5	38.6	0.0000249	0.0396333	21.81	86.44
2	Ra16	307.2	42.9	0.0001155	0.0304477	16.86	51.33	25	D12	278.6	71.0	0.0000286	0.0498177	17.55	87.44
3	Ra24	274.1	76.2	0.0000588	0.0699815	11.81	82.64	26	E5	322.1	27.9	0.0000020	0.0521167	19.01	99.05
4	Ra33	313.6	36.6	0.0000793	0.0429711	15.92	68.42	27	F2	200.4	23.7	0.0001321	0.1060751	7.19	76.26
5	Ra38	293.1	58.5	0.0000607	0.0534537	14.57	77.88	28	F4	304.7	47.3	0.0000318	0.0434895	19.44	84.55
6	Ra39	296.6	53.6	0.0000575	0.0587778	13.67	80.35	29	F6	294.3	35.3	0.0000274	0.0462298	18.84	87.08
7	Ra51	301.3	49.1	0.0000610	0.0358982	19.55	70.18	30	F8	281.8	39.1	0.0000683	0.0581084	13.30	77.29
8	Ra56	264.4	46.3	0.0000551	0.0356912	20.22	72.16	31	F10	336.8	13.56	0.0000297	0.0687451	13.13	90.25
9	Ra65	273.0	77.0	0.0000627	0.0480807	15.69	75.42	32	F12	303.9	46.3	0.0000316	0.0478520	17.94	85.85
10	Ra69	269.7	64.0	0.0000344	0.0287405	26.79	76.98	33	G5	304.7	45.5	0.0000210	0.0640984	14.42	92.45
11	Ra84	266.7	83.3	0.0000335	0.0468970	18.09	84.84	34	H2	288.2	39.6	0.0000793	0.0543175	13.49	73.26
12	A5	306.1	45.9	0.0000371	0.0943537	9.65	91.06	35	H4	195.6	10.8	0.0000293	0.0549856	16.05	88.24
13	B2	257.1	39.2	0.0000249	0.0607969	14.92	90.70	36	H6	308.6	41.4	0.0000648	0.0649589	12.32	80.05
14	B4	277.6	72.4	0.0001108	0.1114198	7.19	80.09	37	H8	290.1	85.1	0.0000192	0.0726639	12.91	93.81
15	B6	283.5	66.5	0.0000948	0.0908322	8.73	79.31	38	H10	311.7	38.4	0.0000327	0.0745807	12.09	90.13
16	B8	303.6	18.4	0.0000158	0.1096541	8.80	96.53	39	H12	287.5	62.6	0.0000485	0.0480971	16.60	79.86
17	B10	300.2	36.8	0.0001424	0.0458039	12.29	56.27	40	I5	289.8	60.8	0.0000514	0.0592454	13.87	82.18
18	B12	312.1	26.6	0.0000267	0.0409332	21.00	85.97	41	J2	306.2	46.9	0.0000703	0.0547603	13.82	75.71
19	C5	260.5	68.8	0.0000464	0.0836252	10.50	87.83	42	J4	289.0	61.0	0.0000412	0.0481283	17.12	82.38
20	D2	248.3	75.5	0.0000717	0.0669828	11.78	78.90	43	J6	273.8	78.0	0.0000306	0.0671046	13.38	89.76
21	D4	245.3	51.6	0.0000237	0.0904840	10.37	93.86	44	J8	297.8	51.9	0.0000313	0.0682151	13.15	89.71
22	D6	278.1	73.5	0.0000267	0.1160328	8.15	94.57	45	J10	308.3	41.7	0.0000594	0.0976939	8.89	86.81
23	D8	307.8	40.9	0.0000769	0.0808097	10.00	80.79	46	J12	300.2	40.4	0.0000211	0.0505795	17.91	90.56

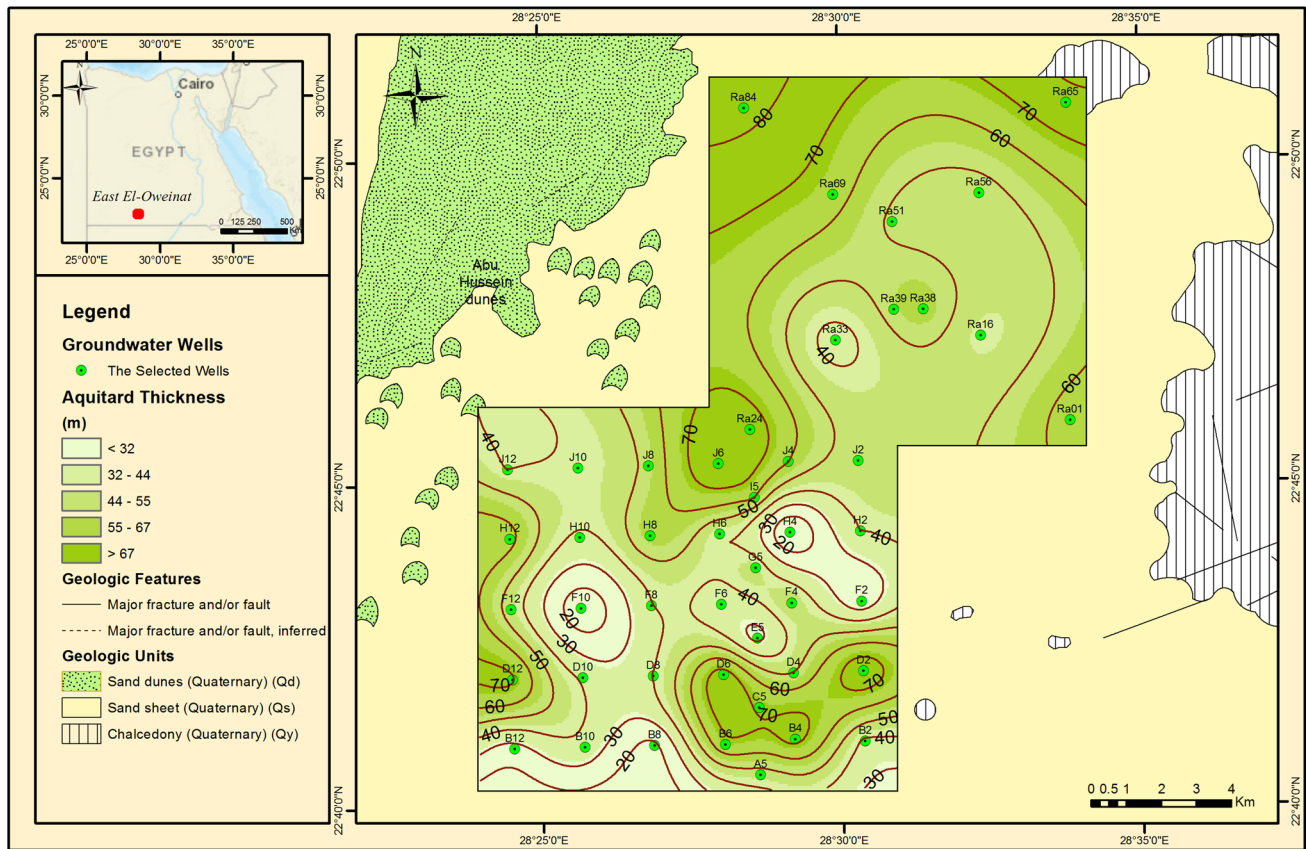


Fig. 5 Isocontour map showing the aquitard thickness in the study area, East El-Oweinat

Some cross sections have been constructed through the studied area to follow up and to delineate the lateral changes of the subsurface lithofacies and thickness of both the aquifer and aquitards. Four cross sections are presented in this study area; two of them are drawn through the E–W direction (Fig. 6), while the others are presented through the N–S direction (Fig. 7).

Sandstone is the dominant composition of the Nubia aquifer, intercalated with thin beds of shales as aquitards (Figs. 6 and 7). The basement rocks are assigned in some wells forming its resting bottom such as B2 well (Fig. 6a).

From studying the cross section A–A', it is indicated that the lateral and vertical distribution of the shale layers 'aquitard' in the E–W direction (Fig. 6a) shows that the shale increases toward the eastern direction, particularly in between B6 and B4 wells. These aquitard layers divide the bulk aquifer into some sub-aquifers, which increase in number toward the eastern wells. In the northern sector, the available aquitard thickness through the C–C' cross section (J12, J10, J8, J6, J4, J2 and Ra01 wells) indicates the presence of some shale lenses in the centre of the studied cross section with the thickest aquitard in the centre (at J6 well, 78.0 m), then decreases slightly to Ra01 well (63.6 m) the eastern parts (Fig. 6b, Table 2).

Through the border of the northern sector and parallel to the A–A' and C–C' cross sections, it is revealed that thickness of the shale layers decreases in the central wells through the northern border of the northern sector in between R65 and R84 wells. The Nubia aquifer indicates a high potential as underground water carrier sequence. Therefore, further exploration for underground water has been conducted with many productive wells to the east of the studied northern sector.

In addition, studying the cross section E–E' revealed that thicknesses of shale beds in the N–S direction through the southern sector (Fig. 7a) are characterised by continuous occurrences along the studied area from the south to the north. The aquitard thickness reaches its maximum value near the western parts of the southern sector of the study area. The aquitard layers divide the aquifer into sub-aquifers, which are continuous along the southern and northern direction, due to the extension of these impervious layers (E–E').

Additional cross section has been studied in the N–S direction through both northern and southern sectors, G–G' (Fig. 7b) passing through Ra69, Ra33, J2, H2, F2, D2 and B2 wells. The basement rocks have been penetrated through B2 and Ra69 wells. The aquitard thickness through this cross section is relatively lower than that through the other cross

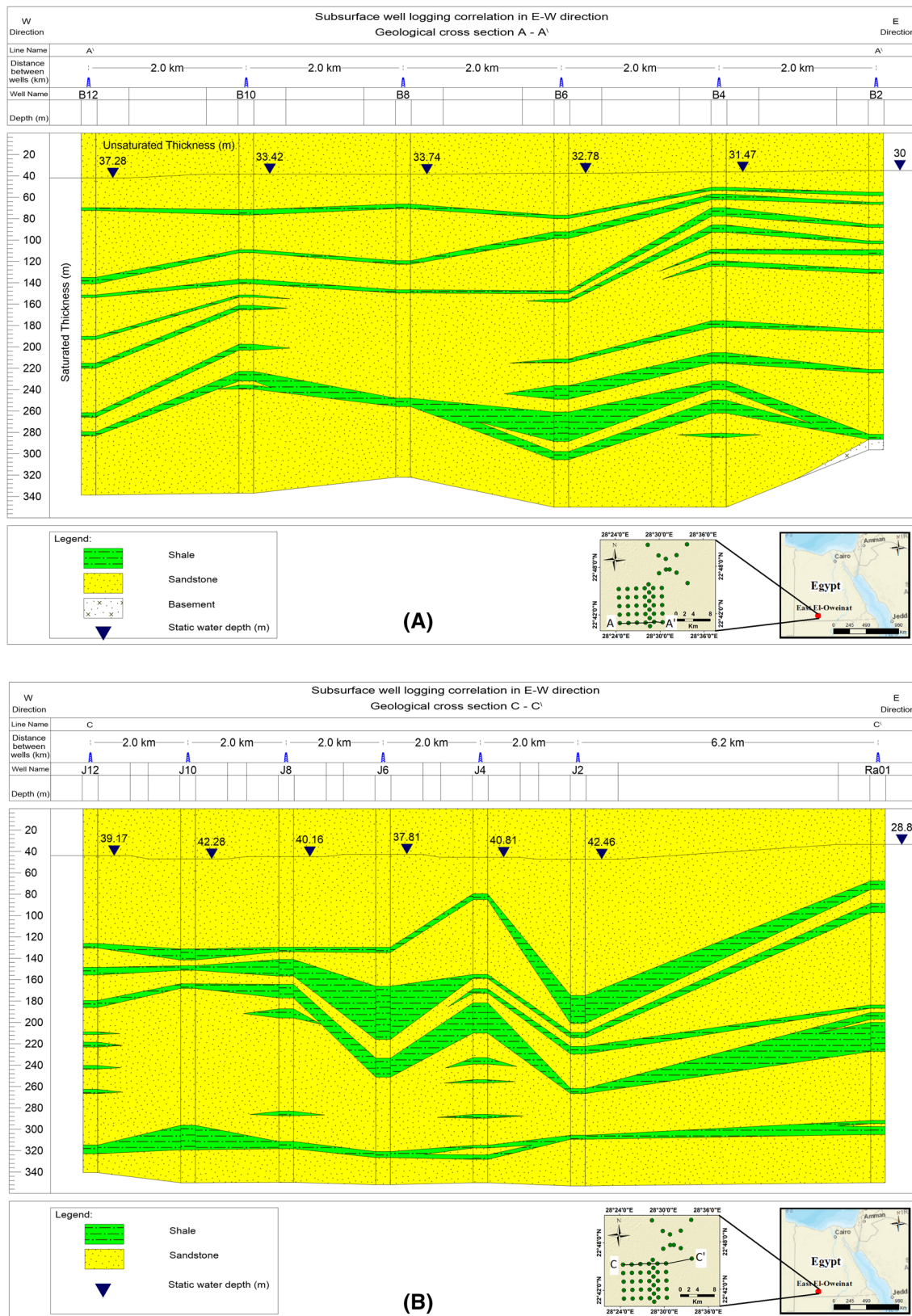


Fig. 6 Subsurface correlation between lithologic units using some Hydrogeological cross sections in the E–W direction through; **a** Southern sector (A–A'), and **b** borders of the southern and the northern sectors (C–C') of the studied area

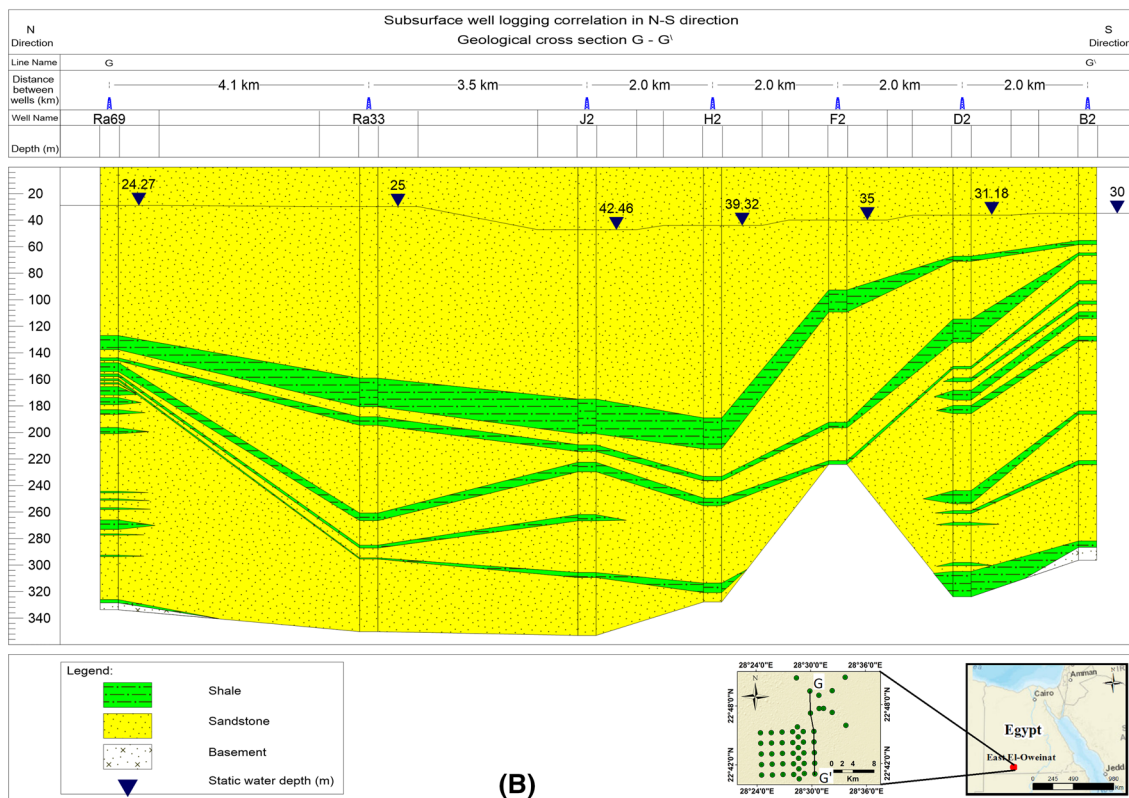
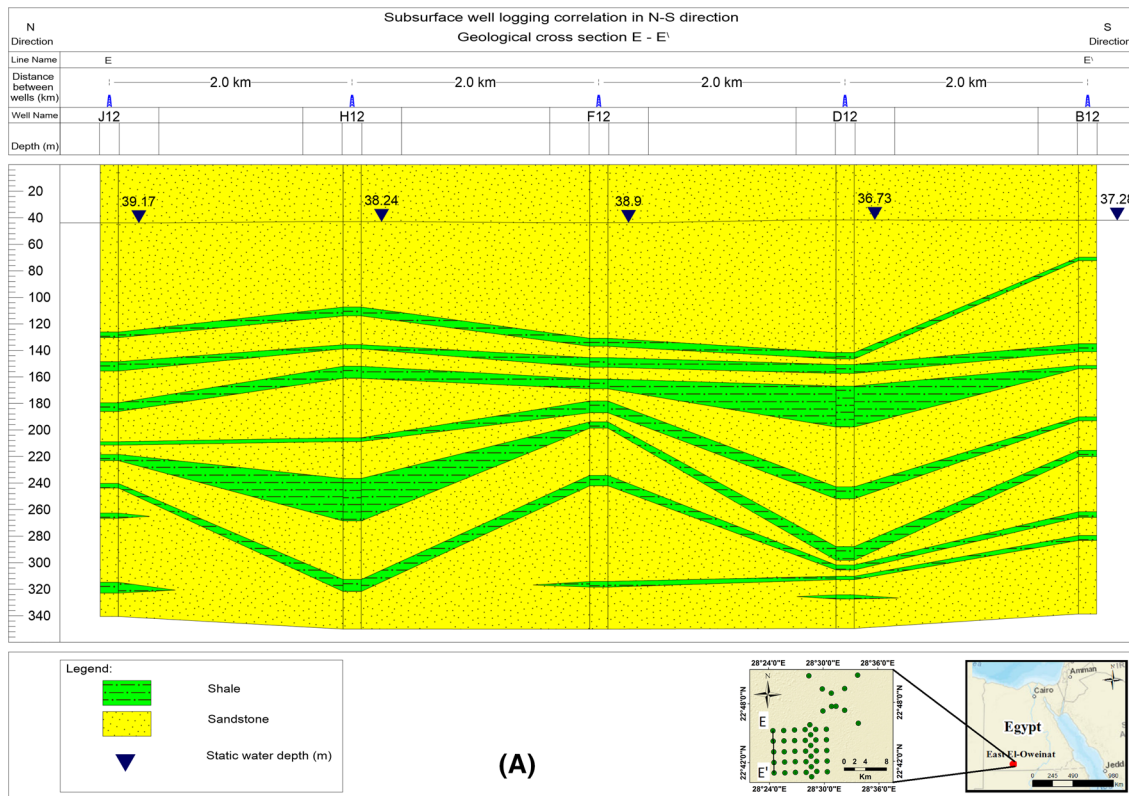


Fig. 7 Subsurface correlation between lithologic units using some Hydrogeological cross sections in the N–S direction through, **a** Southern sector (E–E'), and **b** borders of the southern and the northern sectors (G–G') of the studied area

sections, particularly at the wells in the middle parts of the section including, Ra33, J2, H2, and F2 wells (Table 2). Therefore, it indicates better aquifer thicknesses in the middle parts of the northern sector and the eastern parts of the southern one (Fig. 7b).

In the northern sector, parallel to the cross sections E–E' and G–G' at the eastern border of the northern sector, and in particular between R01 and R65 wells, the available aquitard thickness reveals that the thickness of the shale layers decreases. Therefore, the available data of the aquifer and aquitard thicknesses through the studied cross sections reveal that the potential of the Nubia aquifer increases to the north and east of the northern sector of the study area.

Implementation of the structural regime on the groundwater potential

The structural regime of East El-Oweinat area is dominant by some normal faults trending NNE and NW–SE as shown (Fig. 2). Based on the geoelectrical and magnetic studies carried out by Al Temamy and Barseem (2010) in the study area, it is indicated that the NNE and NW–SE faults as well as some local faults trending E–W affect thickness of the Nubia sandstone as a water-bearing aquifer and striking through basement surface. The difference in the Nubia aquifer thickness is attributed to the presence of a series of minor to major grabens and horsts (Al Temamy and Barseem 2010). The depth to basement along the shallowest horsts in the study area reaches down to a few tens of metres, e.g. around B2 and F2 wells (Figs. 6 and 7). The depth to the basement along the inferred grabens reaches up to 400 m. Consequently, thickness of the Nubia aquifer varies considerably to the north direction. The dominance of the NE–SW trending faults control the alignment of the migration flow lines of the groundwater from the SW to the NE with very low recent annual recharge in comparison to the present extraction rate (Sabet and Zeid 2003; Nabawy et al. 2009, 2010).

Therefore, based on the hydrogeological and structural studies as well as both the pore- and petro-fabrics studies in East El-Oweinat area, the direction of the underground flow has been assigned to fluctuate around the north direction ranging from the NNE and NNW directions (Salem and Pallas 2001; Bakhbaki 2006; Nabawy et al. 2009, 2010, 2015; Nabawy and Géraud 2016). This gives a weight for the future exploration efforts to the north and east of the northern sector of the studied area (Fig. 8).

Step-drawdown test

Applying the step-drawdown test as a tool of the assessment of the Nubia sandstone aquifer is based on determination of the aquifer loss and well loss coefficients (B and C , respectively), as well as the well efficiency and the specific capacity.

1. Aquifer Loss coefficient (B)

From the studied wells, the (B) coefficient ranges from 0.02874 h/m² at Ra69 well to the north and 0.030448 h/m² at R16 well to the east of the northern sector of study area to 0.116 h/m² at D6 well in the central part of the southern sector (Fig. 9, Table 2). However, the variation in the aquifer loss values (B) in the northern sector is relatively low (of average 0.04509 h/m²), while that in the southern sector seems to be relatively high of average (B) value equal to 0.06809 h/m².

In general, the aquifer loss coefficient decreases towards the northeastern direction around Ra56, Ra51 and Ra16 wells, which may be attributed to the lateral change in the lithology of the studied aquifer. The aquifer loss coefficient increases toward the southern direction which may be attributed to better lithologic characteristics.

2. Well Loss coefficient (C)

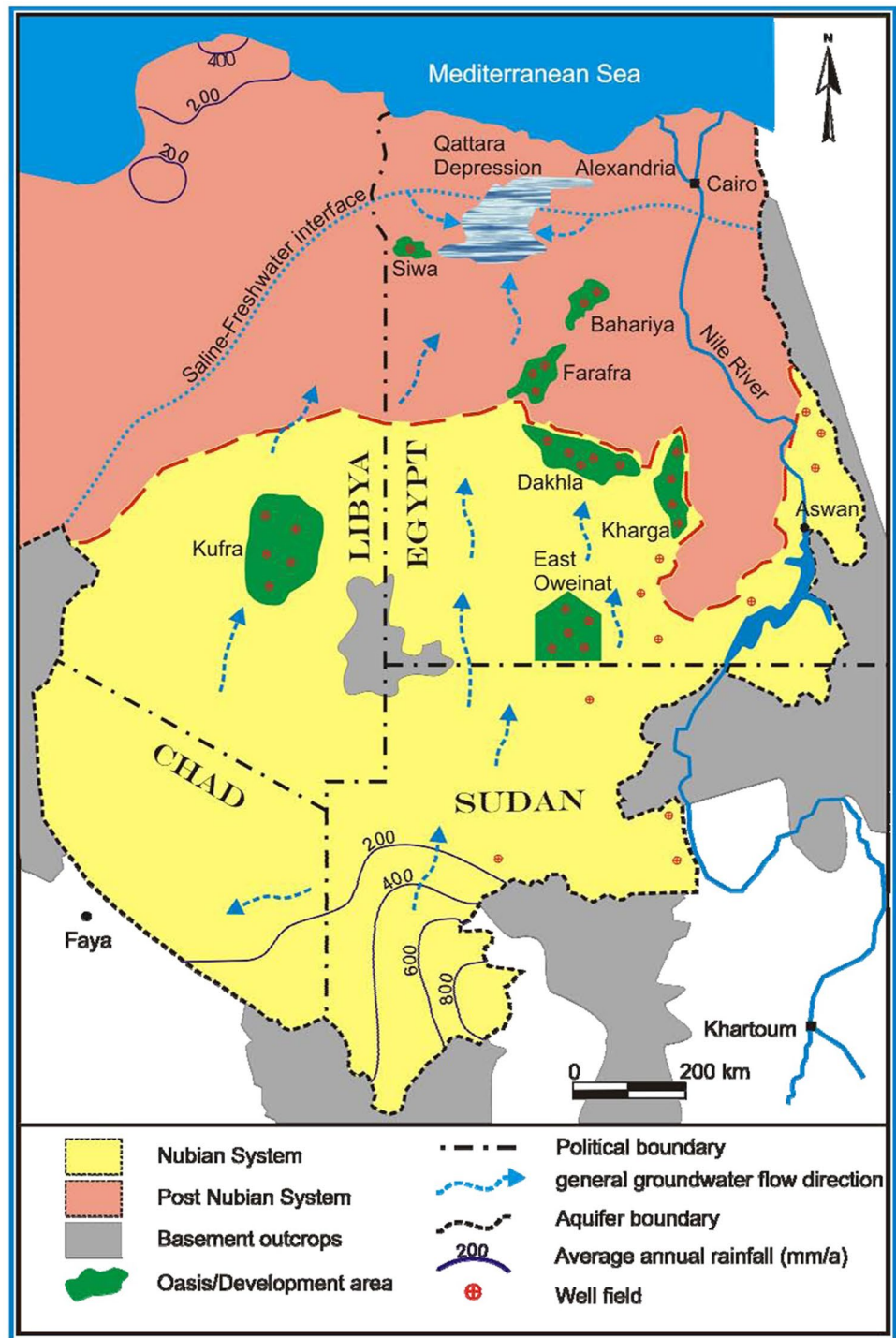
The coefficient (C) varies from 0.000002 h²/m⁵ as a minimum value at E5 well in the central parts of the southern sector to 0.000142 h²/m⁵ at B10 well to the southwest parts of the southern sector of average equals 0.0000478 h²/m⁵ (Fig. 10, Table 2). The relatively high variation of (C) values in the southern sector may be attributed to a lithology variation in the aquifer. The well loss coefficient (C) increases at Ra16 well toward the NE direction, at F2 well in the southeastern parts, and at B10 well in the southern parts.

The maximum (C) value in the northern sector was assigned for Ra16 well ($C=0.0001155$ h²/m⁵) to the SE of the sector and the lowest value at Ra84 well ($C=0.0000335$ h²/m⁵), i.e. (C) values decrease to the northeast parts of average 0.0000619 h²/m⁵ (Fig. 9, Table 2). In general the well loss coefficient values increase at the southwester wells of the northern sector and at the eastern and southern wells of the southern sector as well (Fig. 9).

3. Well Efficiency

The well efficiency has been traced in both the northern and southern sectors as shown in Fig. 11. It is estimated at a discharge rate of 250 m³/h, as recommended as a safe

Fig. 8 A schematic diagram of the Nubia aquifer illustrating the hydrogeological regime which is mostly flowing to the NNE and NNW directions (Bakbakhi 2006; Nabawy et al. 2009)



discharge rate by the general petroleum company GPC (1984). It ranges between 99.05% (at E5 well in the southern sector) and 51.33% (at Ra16 well in the northern sector), with an average values of 74.0% throughout the northern sector and 85.28% in the southern sector of the study area (Fig. 11). Therefore, the estimated efficiency for the productive wells in the southern sector is relatively higher than that for the northern wells.

4. Specific capacity (Sc)

The specific capacity ranges between a maximum value of 26.79 m²/h (at Ra69 well in the northern sector) and a minimum value of 7.19 m²/h (at F2 well in the southern sector) (Fig. 12, Table 2), with averages of 17.30 m²/h for the northern sector and 13.65 m²/h throughout the southern sector (Table 2). The specific capacity decreases toward

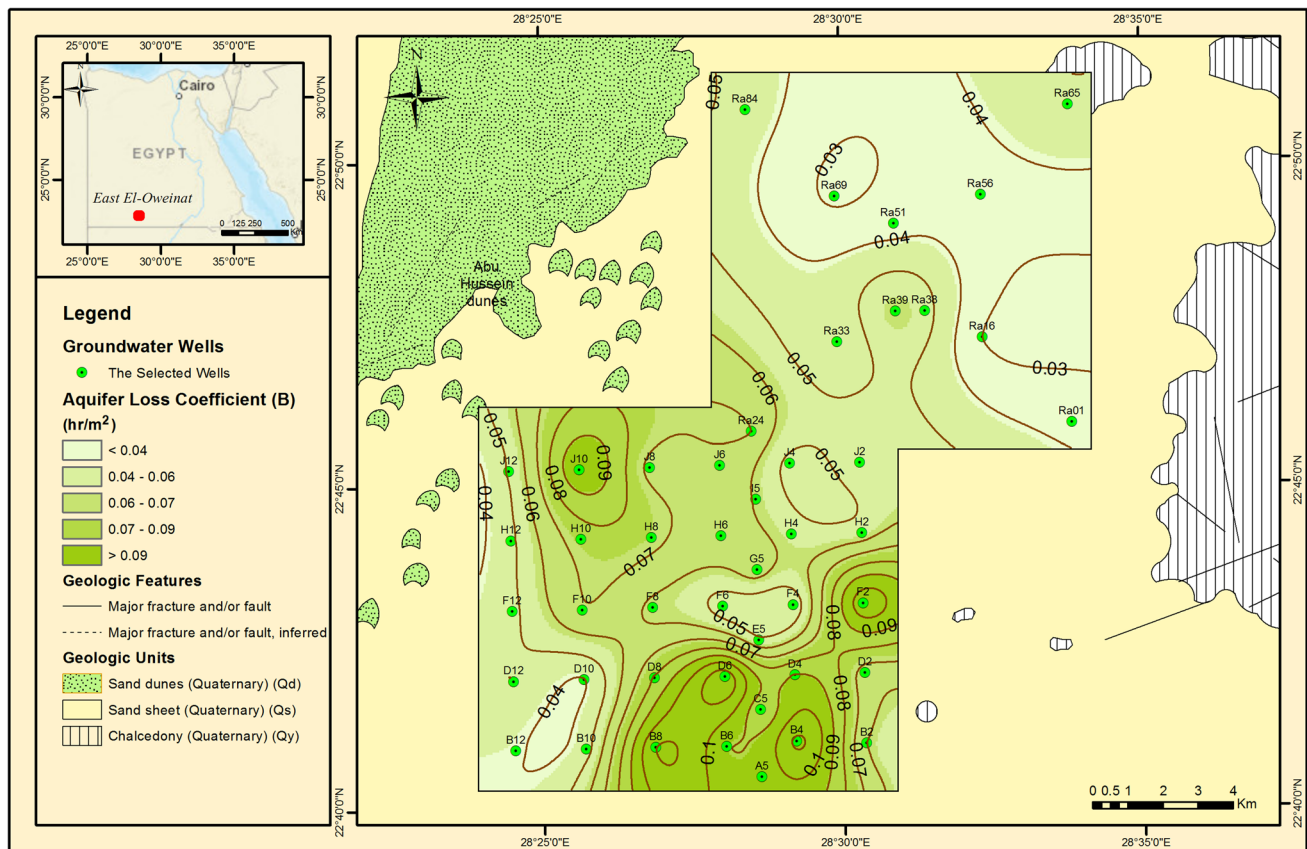


Fig. 9 Isocontour map showing the aquifer loss coefficient (B) in the study area

the southern direction of the study area, e.g., at J10 well ($8.89 \text{ m}^2/\text{h}$), at F2 well ($7.19 \text{ m}^2/\text{h}$), and at B4, D6, B8 and B6 wells (Table 2).

Hydraulic conductivity (K) and transmissivity (T)

For further assessment of the Nubia aquifer in East El-Oweinat area, and since some attention has been paid for future exploration to the north and east of the studied northern sector, the aquifer hydraulic flow and storage properties of the northern 11 wells will be discussed in detail through the following paragraphs.

Based on the total dissolved salts, 'TDS' (340 to 720 mg/l , fresh water), and the electric resistivity of the collected water samples and taking into consideration values of the deep resistivity obtained from log data, effective porosity was calculated (Table 3).

The estimated effective porosity (ϕ_{eff}) values are ranked as good to excellent values (following Levorsen's classification 1967, that has been modified by Nabawy and Al-Azazi 2015) with the minimum value assigned at Ra56 (equals to 17.2%) to the east of the studied area (Fig. 13) and increases

to the NW of the study area with the maximum value equals 31.5% at Ra84 well of average 24.1% (Table 3).

The effective porosity values were then used for estimating the hydraulic conductivity based on Eq. (3). The calculated hydraulic conductivity (K) increases towards the northwest direction with the maximum value (32.9 m/day), assigned at well Ra84, and the least values assigned in the northeastern wells assigned for Ra56 and Ra65 wells (Fig. 14, Table 3).

Finally, the transmissivity (T) has been calculated using Eq. (4), i.e. the estimated values will increase with increasing both the aquifer thickness and the hydraulic conductivity. The transmissivity of the northern wells increase to the NW direction with the maximum value ($10,620 \text{ m}^2/\text{day}$) that assigned for Ra84 well and the least values assigned at the northeastern wells at Ra56 well ($395.2 \text{ m}^2/\text{day}$) (Fig. 15, Table 3).

Aquifer assessment index (AAI)

The aquifer assessment index (AAI) has been introduced in this study to assess and rank the Nubia aquifer in East El-Oweinat area. It is a parameter similar to the RQI that has been long tested successfully by many authors (e.g.

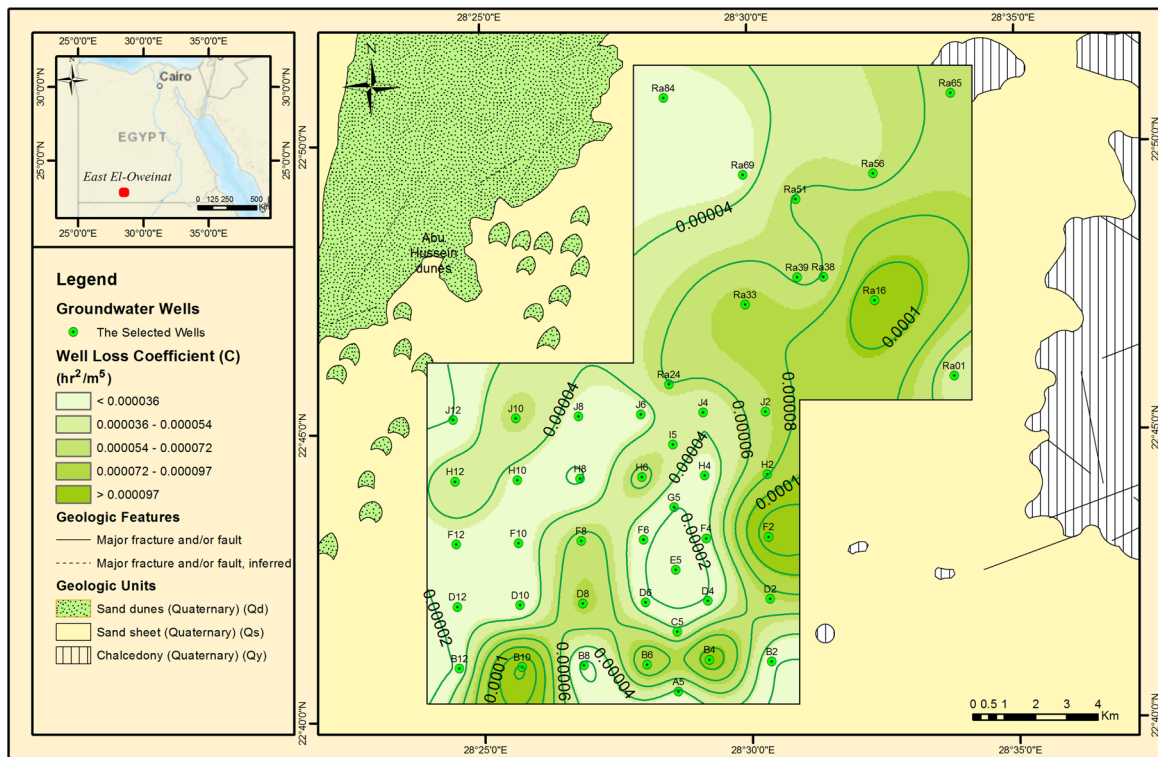


Fig. 10 Isocontour map showing the well loss coefficient (C) in the study area

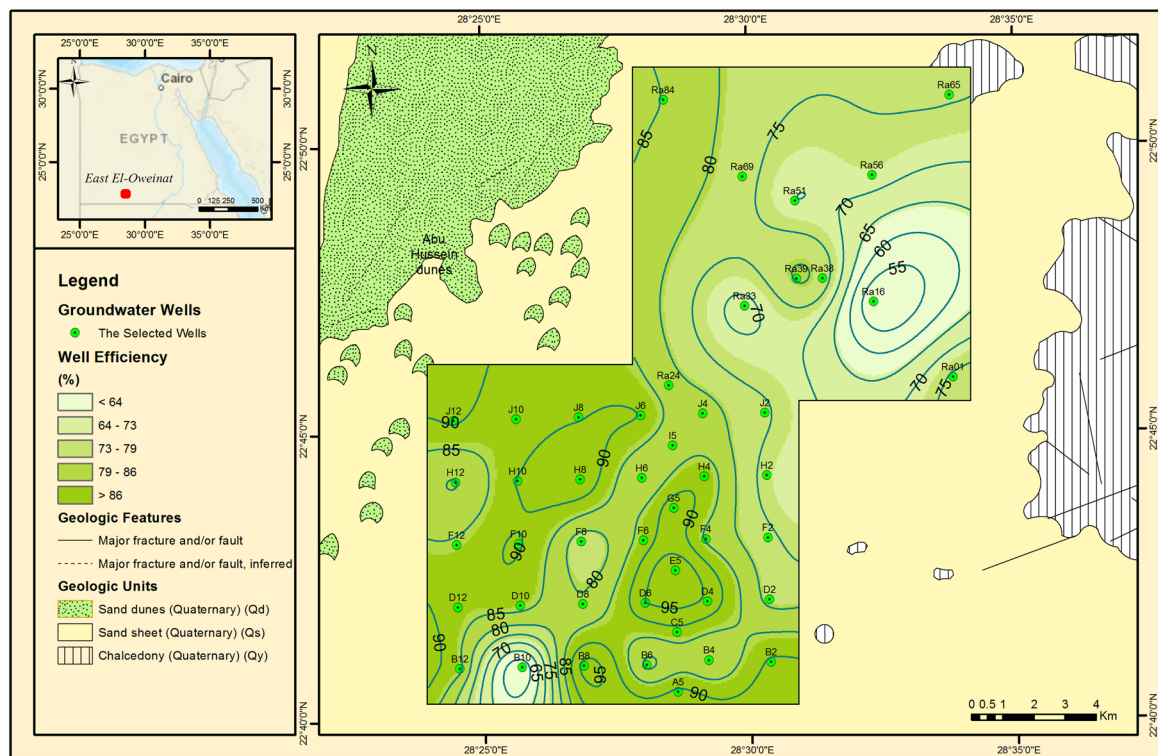


Fig. 11 Isocontour map showing the well Efficiency of the studied wells at discharge rate 250 m³/h, East El-Oweinat area

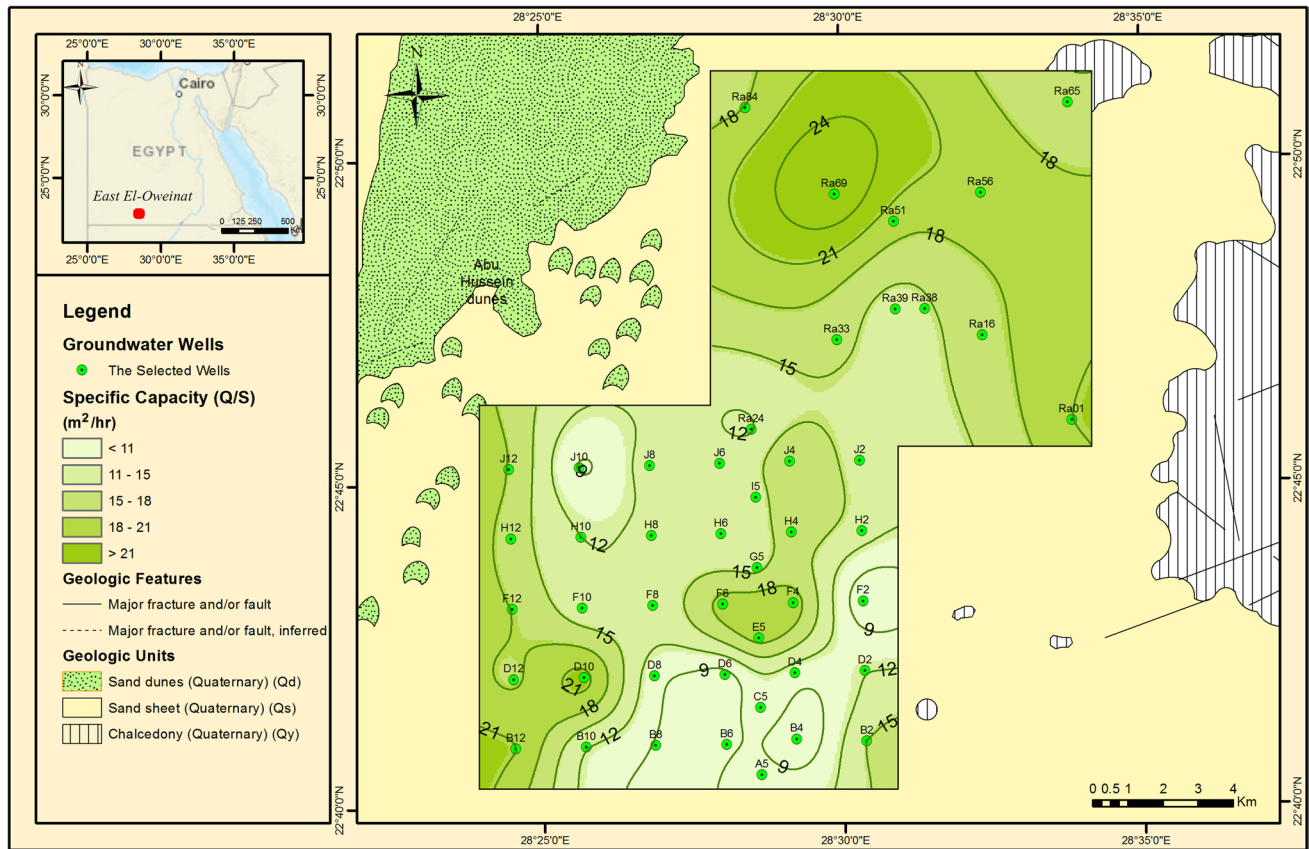


Fig. 12 Isocontour map showing the specific capacity of the studied wells at discharge rate 250 m³/h, East El-Oweinat area

Table 3 The total dissolved salts (TDS), true electric resistivity (Rt), aquifer electric conductivity (Ec), formation water resistivity (R_w), effective porosity (∅_{eff}), hydraulic conductivity (K), transmissivity (T), permeability (k) and aquifer assessment index (AAI) of the studied wells in the northern sector of the study area in east El-Oweinat area, SW Egypt

Well name	TDS mg/l	EC μ mhos/cm	R _w Ohm m	R _t Ohm m	∅ _{eff} %	K m/day	H m	T m ² /day	k μm ²	AAI μm
Ra01	830	1354	7.39	78.05	22.6	4.56	286.4	1466.0	9.67	6.54
Ra16	680	1092	9.16	83.50	24.3	6.70	307.2	2102.0	14.2	7.65
Ra24	710	1330	7.52	88.62	21.4	3.50	274.1	1126.9	7.42	5.89
Ra33	720	1156	8.65	75.71	24.8	7.50	313.6	2438.2	15.9	8.01
Ra38	720	1150	8.70	91.29	22.7	4.64	293.1	1513.4	9.84	6.58
Ra39	640	1039	9.62	86.14	24.6	7.05	296.6	2296.1	14.9	7.80
Ra51	520	805	12.4	111.3	24.6	7.03	301.3	2297.3	14.9	7.78
Ra65	680	1086	9.21	103.6	21.9	3.91	264.4	1281.9	8.29	6.15
Ra56	680	1088	9.20	168.1	17.2	1.37	273.0	395.21	2.91	4.11
Ra69	460	705	14.2	89.42	29.3	20.1	269.7	6214.9	42.6	12.1
Ra84	340	496	20.2	109.8	31.5	32.9	266.7	10620	69.8	14.9

Amaefule et al. 1993; Tiab and Donaldson 1996; Al-Dhafeeri and Nasr-El-Din 2007; Soto et al. 2010; Nabawy and Al-Azazi 2015; Benzagouta 2015a, b; El Sharawy and Nabawy 2016a, b; Nabawy and Barakat 2017; Al-Rbeawi and Kadhim 2017; El Sharawy and Nabawy 2018; Nabawy

et al. 2018a, b; Riazi 2018). For the present study it varies between 4.11 μm at Ra56 well in the northeastern parts of the northern sector and 14.9 μm at Ra84 well in the southwestern parts of the northern sector (Table 3, Fig. 16).

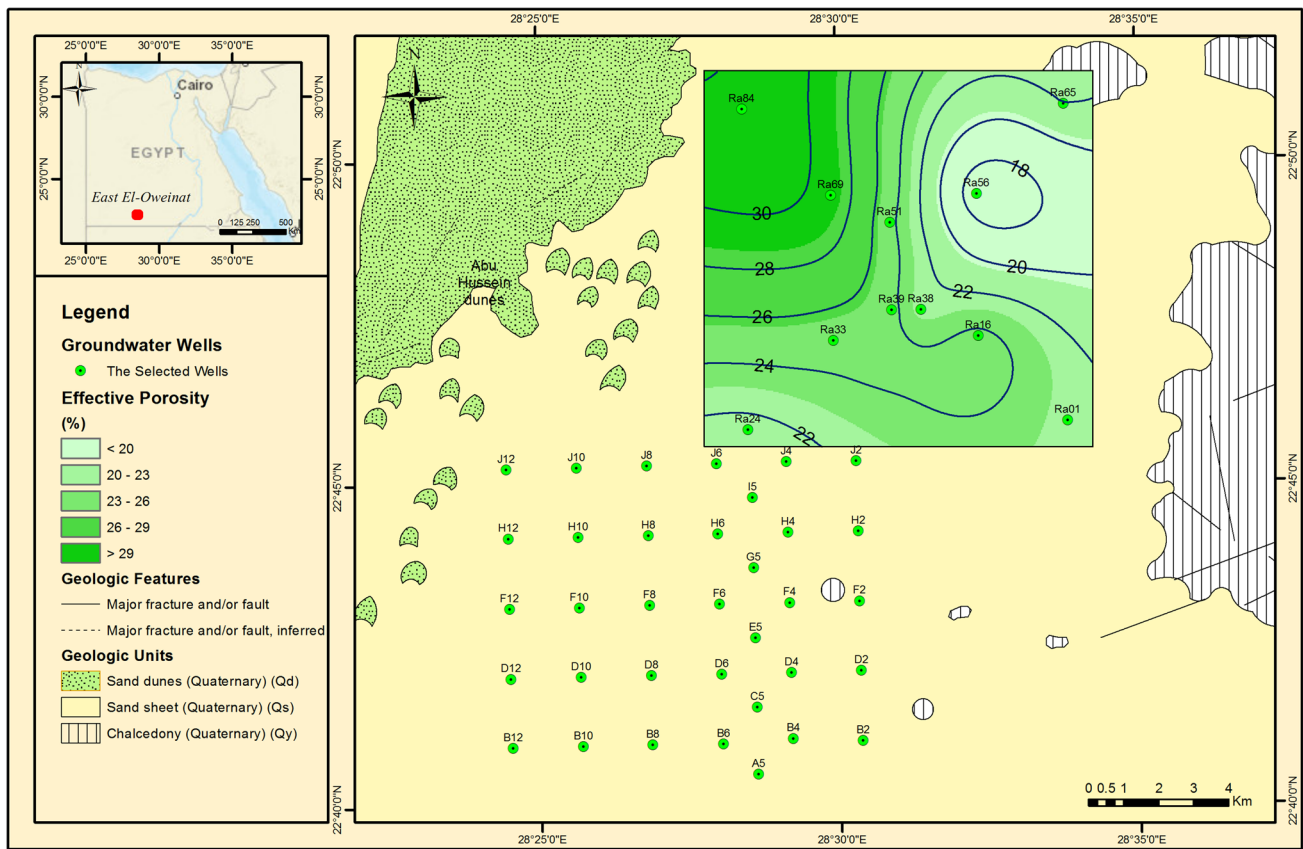


Fig. 13 Isocontour map showing the effective porosity of the studied wells in the northern sector of the study area, East El-Oweinat area

General discussion

Aquifer characterization and assessment is often based on studying the hydrogeological setting including thickness of both the aquifer and the aquitard which seem to increase in the southern sector of the studied wells with relatively lower aquifer and higher aquitard thicknesses to the northern and eastern borders of the northern sector (Figs. 4 and 5). However, since the areas surrounding the southern province have been already cultivated and since the main activities will be devoted to the areas in around the northern sector, the present study pays more attention to the northern sector. The available data in the southern sector have been used for correlation with the northern wells and to complement with the whole hydrogeological regime in East El-Oweinat area.

Lithology of the studied aquifer has been described as a sandstone sequence with some intercalations of shales. However, though the lithology seems to be the same for the aquifer, many literatures referred to some variation in the sand size of the Nubia aquifer from medium to coarse sandstones and to the presence of some diagenetic cement including silica cement, clay minerals and iron oxides due to the prolonged periods of diagenesis and arid climates (Nabawy et al. 2009, 2010; Nabawy and Géraud 2016). The slight

differences in the cement material and the grain size leads to a great difference in both the pore and grain fabrics and, therefore, in the hydraulic properties of the studied aquifer (Nabway and Kassab 2014; Nabawy 2015; Nabawy et al. 2015). Lithology of the studied aquifer plays a significant role in increasing the aquifer loss (*B*), due to the migration of fine particles which may clog out the screens during flow out of the aquifer. In addition, the invasion of the drilling fluids can play an additional significant role in increasing the aquifer loss, where the drilling mud reduces the permeability in around the borehole well (Poehls and Gregory 2009). No relationship can be established between the aquitard thickness and the (*B*) factor for both sectors which indicates that it may be affected by the well design and the degree of well development rather than the aquifer properties and shale layers.

On the other side, the increase in the well loss coefficient (*C*) is accompanied with decrease of the aquitard thickness for the northern wells with no relationship assigned for the southern wells (Fig. 17) which may indicate more effect for the well design in the southern wells.

Therefore, for the present study the well design seems to have a significant effect on both (*B*) and (*C*) coefficients rather than the aquitard thickness. The improper well

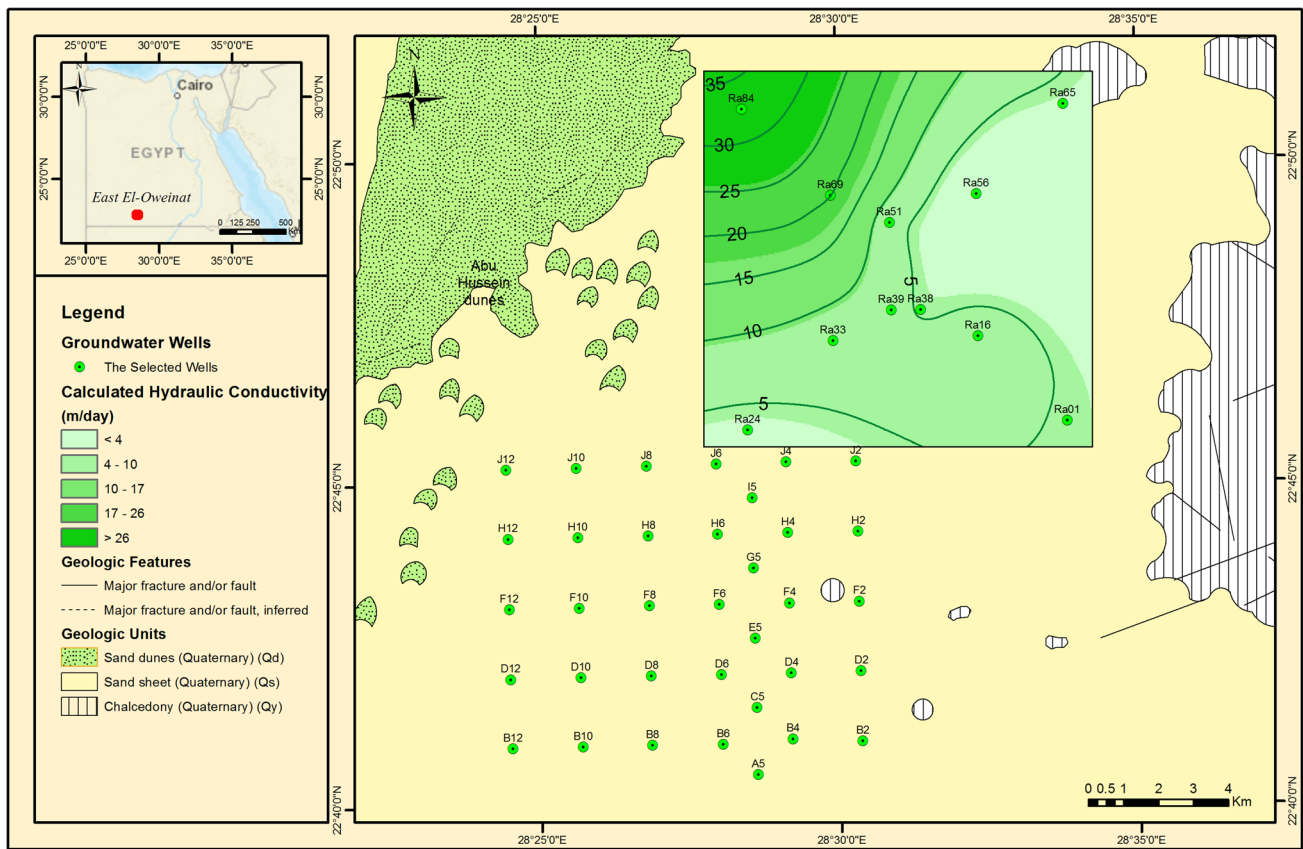


Fig. 14 Isocontour map showing the calculated hydraulic conductivity in the northern sector of the study area, East El-Oweinat area

design by putting the well screen in front of shale layers or sand layers of fine sediments may greatly affect (B) and (C) values, where the fine sediments help in clogging the screen slots and increase the well loss. So, it is advisable to cover the well screen with “wire mesh” in some wells. Also, using a dispersing agent of sodium hexametaphosphate (SHMP) is sometimes useful to easily remove the effect of drilling mud, that reduces the aquifer quality and increases the well loss.

A perfectly efficient well, with perfect well screen and where the water flows inside the well in a frictionless manner would have 100% well efficiency. Unfortunately, the well efficiency is hard to be compared between wells because it depends on the well design as well as the characteristics of the aquifer too (the same amount of well losses compared to a more transmissive aquifer would give a lower efficiency).

The well efficiency of the studied wells increases toward the northwestern direction around Ra84 well, with the decrease of the well loss coefficient (C) (Figs. 9 and 10), while it decreases to the southeast with the increase of the (C) values (Figs. 9 and 10). For the southern sector, the well efficiency decreases to the east and south direction with increasing the (C) factor. It seems that the well efficiency

is controlled mostly by the loss coefficient (C) as a main controlling factor (Fig. 18).

It seems that the hydraulic parameters, including porosity, hydraulic conductivity and transmissivity, play additional role in increasing the well efficiency, where the hydraulic parameters increase to the northwest direction around the Ra84 well (Figs. 10, 12, 13 and 14). The aquifer thickness is a main contributor to the transmissivity; i.e. it is reasonably a main contributor to the well efficiency.

Therefore, both the aquifer and aquitard thicknesses of the studied wells are main contributors to the well efficiency in a direct or indirect contribution as well as the hydraulic parameters and the well design.

Finally, applying the AAI parameter to assess the Nubia aquifer supports the conclusion that the best aquifer quality is assigned to the northwestern direction of the studied wells, where the AAI values vary in general between 4.11 μm and 14.9 μm with most values more than 6.0 μm . To rank the studied aquifer and following the classification for reservoirs introduced by Nabawy and Al-Azazi (2015), we applied the following classification:

- Rank-1, Excellent Aquifer, $\text{AAI} > 2.00 \mu\text{m}$,
- Rank-2, Excellent Aquifer, $1.00 < \text{AAI} \leq 2.00 \mu\text{m}$,

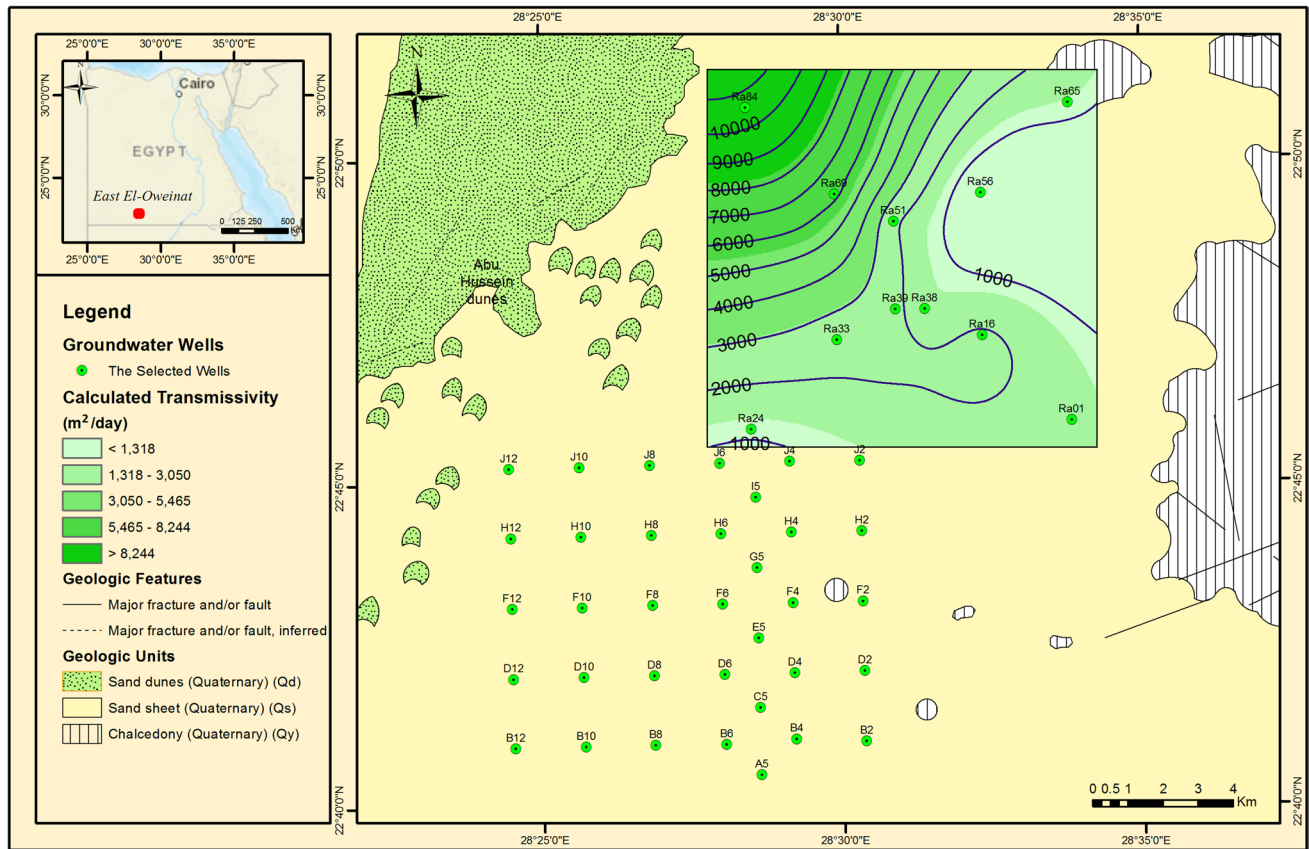


Fig. 15 Isocontour map showing the calculated transmissivity in the northern sector of the study area, East El-Oweinat

- Rank-3, Excellent Aquifer, $0.50 < AAI \leq 1.00 \mu m$,
- Rank-4, Excellent Aquifer, $0.25 < AAI \leq 0.50 \mu m$,
- Rank-5, Excellent Aquifer, $0.10 < AAI \leq 0.25 \mu m$, and
- Rank-1, Excellent Aquifer, $0.00 < AAI \leq 0.10 \mu m$.

Based on this classification, the studied Nubia aquifer is ranked as excellent aquifer at the different wells. To test the main attributors to the AAI parameter and the high ability of the AAI to be used as a sole representative parameter for the aquifer quality, it is plotted as a function of the main aquifer parameters porosity, hydraulic conductivity, and transmissivity (Fig. 19). It is indicated that the AAI parameter has an excellent relationships with its contributor including porosity ($R^2 = 0.981$, Fig. 19a), hydraulic conductivity ($R^2 = 0.999$, Fig. 19b) and transmissivity ($R^2 = 0.996$, Fig. 19c). Therefore, the AAI parameter could be used successfully as a quality parameters instead of the common aquifer quality parameters (\emptyset , K , and T) for ranking the studied aquifer

Conclusions

The Nubia aquifer in East El-Oweinat area has good hydrogeological setting and hydraulic properties. It is characterised by good aquifer thickness that reaches up to 336 m with relatively low aquitard thickness. It is composed of medium- to coarse-grained sandstones intercalated with same shale beds. The aquifer sequence suffered from a long period of a dominant arid diagenetic history that helped in increasing the storage capacity and enhanced the hydraulic parameter of the Nubia aquifer.

The step-drawdown test has been applied to underground wells in the area under assessment for two groups of wells: the first one is situated in a southern sector, used for correlation and tracing, and the second group is situated in a northern sector. From the step-drawdown test, it is concluded that the well efficiency is controlled mostly by the well loss coefficient, (C) and both the aquifer and aquitard thicknesses as well. The improper well design is

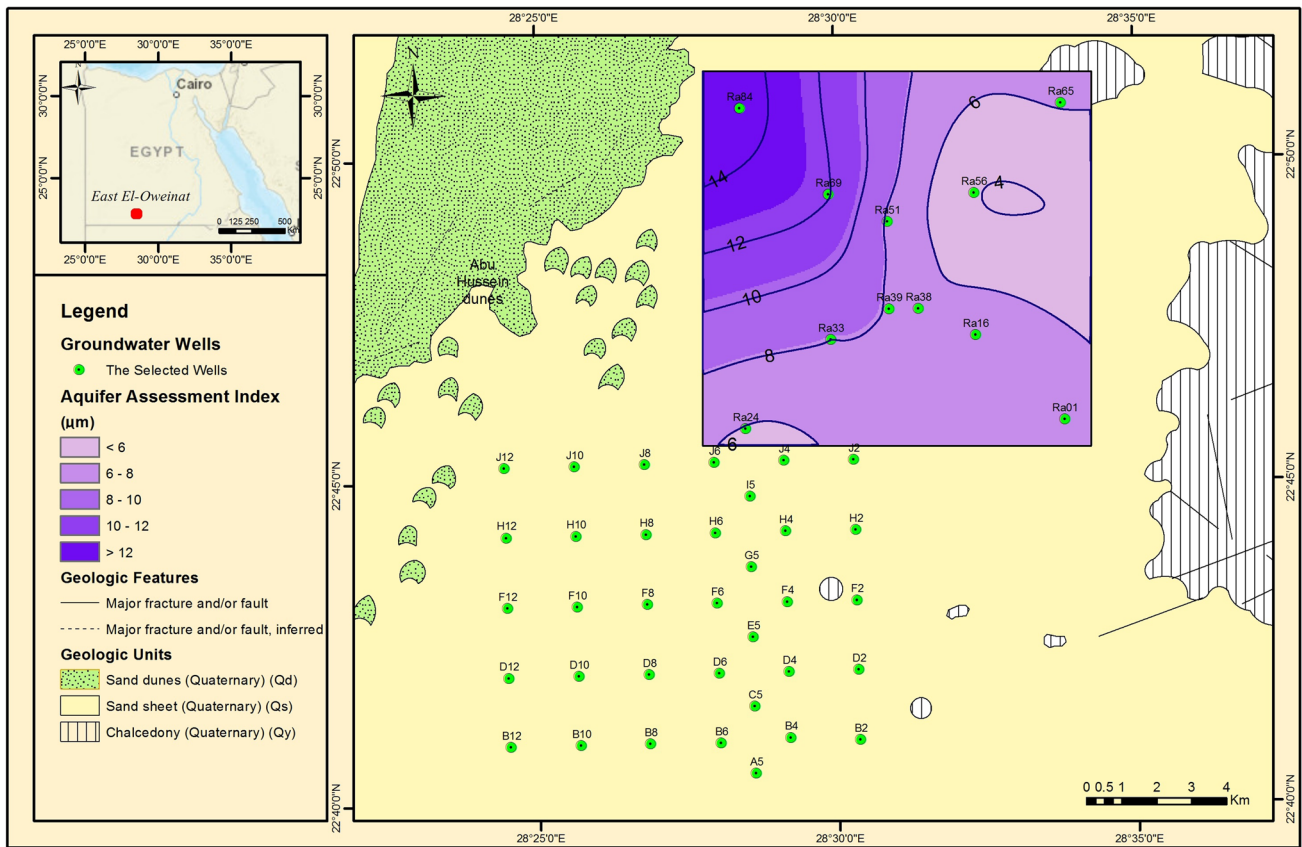


Fig. 16 Isocontour map showing the aquifer assessment index (AAI) in the northern sector of the study area, East El-Oweinat

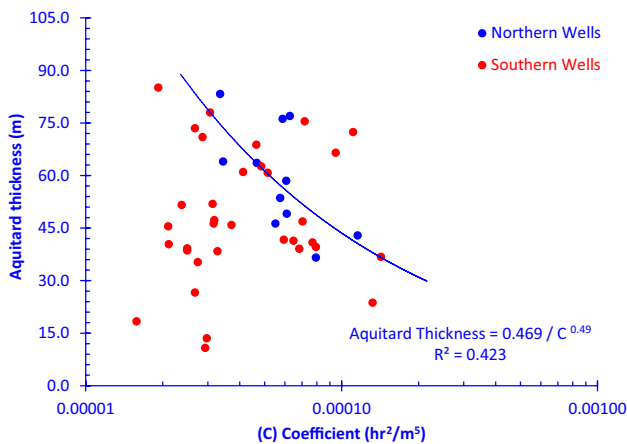


Fig. 17 Plotting the (C) factor as a function of the aquitard thickness for the studied wells, East El-Oweinat

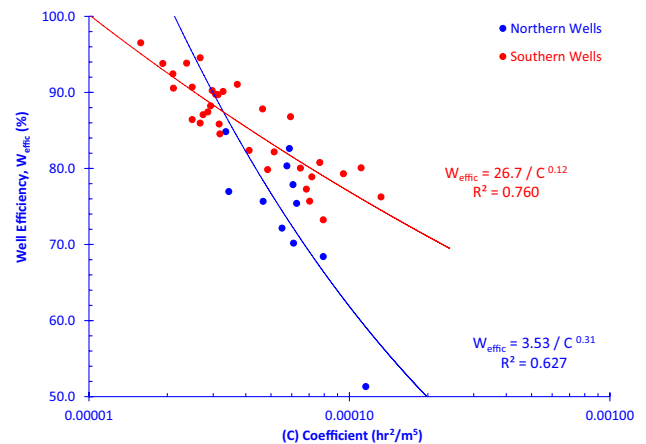


Fig. 18 Plotting the (C) factor as a function of the well efficiency for the studied wells, East El-Oweinat

additional controlling factor reducing the well efficiency and causes a disturbance for the relationship between the hydraulic parameters and the well efficiency, i.e. unexpected low well efficiency is obtained for a groundwater well with good hydraulic properties. Applying the aquifer

assessment index (AAI) as a supplementary parameter for porosity, hydraulic conductivity and transmissivity of the aquifer indicates an excellent aquifer quality at the different wells.

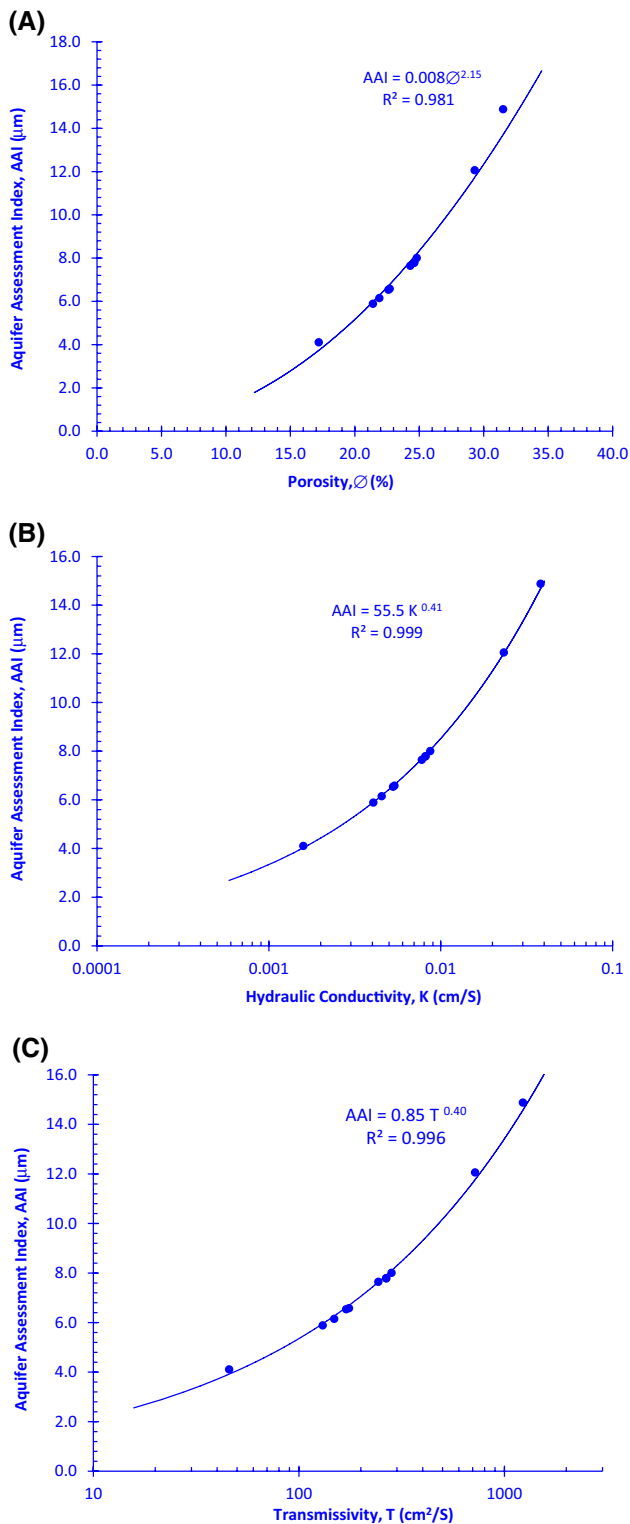


Fig. 19 Plotting the AAI parameter as a function of the main aquifer assessment parameters including, **a** porosity, **b** hydraulic conductivity, and **c** transmissivity

The structural regime controls the underground water flow and introduces permeable pathways striking towards the north direction and NNE direction.

Further exploration for groundwater is recommended and encouraged in a direction to further localities to the north and east of the study area.

Acknowledgements Thanks are due to the General Company for Research and Groundwater “REGWA” for releasing some of the data. The authors would like also to express their deepest gratitude to Geologist Awsy Khalil Swailam, Chairman of REGWA and Dr. Amal Hosny Esmail, Head of Executive Sector, Director of Training Department for their helpful spirit in providing the necessary information. Special thanks are due to the great efforts of the Editor-in-Chief Prof Dr James LaMoreaux and the anonymous reviewers whose constructive comments greatly contributed to and enhanced the quality of the manuscript.

References

Al Temamy AMM, Barseem MSM (2010) Structural impact on the groundwater occurrence in the Nubia sandstone aquifer using geomagnetic and geoelectrical techniques, Northwest Bir Tarfawi, East El Oweinat area, Western Desert, Egyptian Geophysical Society. *EGS J* 8(1):47–63

Al-Dhafeeri AM, Nasr-El-Din HA (2007) Characteristics of high permeability zones using core analysis, and production logging data. *J Petrol Sci Eng* 55(1–2):18–36

Al-Rbeawi S, Kadhim F (2017) The impact of hydraulic flow unit & reservoir quality index on pressure profile and productivity index in multi-segments reservoirs. *Petroleum* 3(4):414–430

Amaefule J, Altunbay M, Tiab D, Kersey D, Keelan D (1993) Enhanced reservoir description using core and log data to identify hydraulic flow units and predict permeability in uncored intervals/wells. *SPE* 26436:205–220

Bakhbakhi M (2006) Nubian sandstone aquifer system. In: Non-renewable groundwater resources, a guide book on socially-sustainable management for water policy makers. In: Foster S, Loucks DP (eds) IHP-VI, series on ground water, vol 10. United Nations Educational, Scientific and Cultural Organization, Paris, 100p

Benzagouta MS (2015a) Reservoir characterization: evaluation for the channel deposits sequence—upper part using scanning electron microscope (SEM) and mercury injection (MICP): case of tight reservoirs (North Sea). *J King Saud Univ Eng Sci* 27(1):57–62

Benzagouta MS (2015b) The use of polar angle, polar arm and other physical attributes in rock characterization. *J King Saud Univ Eng Sci* 27(2):232–237

Bierschenk WH (1963) Determining well efficiency by multiple step-drawdown tests. *Intern Assoc Sci Hydrol Publ* 64:493–507

Bierschenk WH, Wilson GR (1961) The exploitation and development of ground water resources in Iran. *Int Assoc Sci Hydrol Publ* 57:607–627

Bruin J, Hudson HE (1955) Selected methods for pumping test analysis. *Ill State Water Surv Rep Investig* 25:29–37

CONOCO (Continental Oil Company) (1987) Stratigraphic lexicon and explanatory notes to the geologic map of Egypt 1:500,000. In: Hermina, Maurice, Eberhard, List FK (eds)

El Sharawy MS, Nabawy BS (2016a) Determination of electrofacies using wireline logs based on multivariate statistical analysis for the Kareem Formation, Gulf of Suez, Egypt. *Environ Earth Sci* 75(21):1394

- El Sharawy MS, Nabawy BS (2016b) Geological and petrophysical characterization of the lower senonian matulla formation in Southern and Central Gulf of Suez, Egypt. *Arab J Sci Eng* 41(1):281–300
- El Sharawy MS, Nabawy BS (2018) Determining the porosity exponent m and lithology factor a for sandstones and their control by overburden pressure: a case study from the Gulf of Suez, Egypt. *AAPG Bull* 102(9):1893–1910
- GPC General Petroleum Company (1984) Hydro-agriculture study of East El-Oweinat region, Western Desert, Egypt. GPC, Ministry of Petroleum, A.R.E. 3-A:178p
- Guyod H (1966) Interpretation of electric and gamma ray logs in water wells. *Log Analyst* 6(5):29–44
- Hantush MS (1964) Hydraulics of wells. In: Chow VT (ed) *Advances in hydro-science*, vol 1. Academic Press, New York, pp 281–432
- Hendriks F (1988) Evolution of the depositional environments of southwestern Egypt during the Cretaceous and Lower tertiary. *Belliner Geowiss Abhandlungen* 75(1):49–82
- Issawi B (1973) Nubia sandstone type section. *Bull AAPG* 57:741–745
- Issawi B, Jux U (1982) Contribution to the stratigraphy of Paleozoic rocks in Egypt: geological survey of Egypt. *Cairo* 64:28p
- Issawi B, Osman RA (1993) Tectonic-sedimentary synthesis of Paleozoic-Cretaceous clastics, SW Aswan, Egypt. *J Sedimentol Soc Egypt* 1:11–22
- Jacob CE (1947) Drawdown test to determine effective radius of artesian well. *Trans ASCE* 112:1047–1070
- Jacob CE (1950) Flow of ground water. Chapter 5 in *Engineering hydraulics*. In: Rouse H (ed) Wiley, New York, pp 321–386
- Kawecki MW (1995) Meaningful Interpretation of step-drawdown tests. *Ground Water* 33(1):23–32
- Klitzsch E (1979) Major subdivisions and Depositional Environments of Nubia Strata, Southwestern, Egypt. *Egypt Bull Am Ass Petrol Geol Tulsa* 63(6):967–974
- Klitzsch E (1984) Northwestern Sudan and bordering areas: geological development since cambrian time. Results of the special research project Arid Areas, Berlin, pp 23–47
- Kruseman GP, de Ridder NA (1994) Analysis and evaluation of pumping test data, 2nd edn. Publication 47, International Institute for Land Reclamation and Improvement, Wageningen, The Netherlands, 370p
- Kruseman GP, de Ridder NA (2000) Analysis and evaluation of pumping test data, 2nd edn. International Institute for Land Reclamation and Improvement, Wageningen. The Netherlands, 377p
- Levorsen AI (1967) *Geology of petroleum*. WH Freeman Company, San Francisco
- Marotz G (1968) *Technische grundlageneiner wasserspeicherung imm natuerlichen untergrund habilitationsschrift*. Universitat Stuttgart
- Mogg JL (1969) Step-drawdown test needs critical review. *Ground Water* 7(1):28–34
- Nabawy BS (2014) Estimating porosity and permeability using digital Image analysis (DIA) technique for highly porous sandstones. *Arab J Geosci* 7(3):889–898
- Nabawy BS (2015) Impacts of the pore- and petro-fabrics on porosity exponent and lithology factor of Archie's equation for carbonate rocks. *J Afr Earth Sci* 108:101–114
- Nabawy BS, Al-Azazi NAS (2015) Reservoir zonation and discrimination using the routine core analyses data: the upper Jurassic Sab'atayn sandstones as a case study, Sab'atayn basin, Yemen. *Arab J Geosci* 8(8):5511–5530
- Nabawy BS, Géraud Y (2016) Impacts of pore- and petro-fabrics, mineral composition and diagenetic history on the bulk thermal conductivity of sandstones. *J Afr Earth Sci* 115:48–62
- Nabawy BS, Rochette P, Géraud Y (2009) Petrophysical and magnetic pore network anisotropy of some cretaceous sandstone from Tushka Basin, Egypt. *Geophys J Int* 177(1):43–61
- Nabawy BS, Rochette P, Géraud Y (2010) Electric pore fabric of the Nubia sandstones in south Egypt: characterization and modelling. *Geophys J Int* 183:681–694
- Nabawy BS, Sediek KN, Nafee SA (2015) Pore fabric assignment using electrical conductivity of some Albian-Cenomanian sequences in north Eastern Desert, Egypt. *Arab J Geosci* 8(8):5601–5615
- Nabawy BS, Basal AMK, Sarhan MA, Safa MG (2018a) Reservoir zonation, rock typing and compartmentalization of the Tortonian-Serravallian sequence, Temsah Gas Field, offshore Nile Delta, Egypt. *Mar Pet Geol* 92:609–631
- Nabawy BS, Rashed MA, Mansour AS, Afify WSM (2018b) Petrophysical and microfacies analysis as a tool for reservoir rock typing and modeling: Rudeis Formation, off-shore October Oil Field, Sinai. *Mar Pet Geol* 97:260–276
- Nabawy BS, Kassab MA (2014) Porosity-reducing and porosity-enhancing diagenetic factors for some carbonate microfacies: a guide for petrophysical facies discrimination. *Arab J Geosci* 7(11):4523–4539
- Nabawy BS, Barakat MK (2017) Formation evaluation using conventional and special core analyses: belayim Formation as a case study, Gulf of Suez, Egypt. *Arab J Geosci* 10(2)
- Nour SE (1979) Preliminary investigations of groundwater and soil resources in East Oweinat area, Western Desert, Egypt. The General Petroleum Company (GPC). Report, Cairo University, 64p
- Nour S (1996) Groundwater potential for irrigation in the East Oweinat area, western desert, Egypt. *Environmental Geology* 27(3):143–154
- Poehls DJ, Gregory JS (2009) *Encyclopedic dictionary of hydrogeology*. Academic Press, Boca Raton, p 517
- Riazi Z (2018) Application of integrated rock typing and flow units identification methods for an Iranian carbonate reservoir. *J Pet Sci Eng* 160:483–497
- RIGW (2008) Research institute for ground water. Internal report about the potentiality of groundwater in East El-Oweinat area. Ministry of Water Resources and Irrigation, Water Resources Research Institute, Egypt. Interior unpublished report, 18p
- Sabet SS, Zeid AM (2003) Contributions to the hydrogeology of Nubian sandstone aquifer in East El-Oweinat area, South Western Desert, Egypt. *Isot Rad Res* 33:11–177
- Said R (1962) *Geology of Egypt*. Elsevier, Amsterdam, New York, pp 218–287
- Salem O, Pallas P (2001) The Nubian sandstone aquifer system (NSAS). In: International shared (transboundary) aquifer resources management—their significance and sustainable management. In: Puri S (ed) IHP-VI, IHP non serial publications in hydrology. UNESCO, Paris, pp 41–44
- Soto RS, Arteaga D, Hidalgo CM, Rodriguez F (2010) Pore-type determination from core data using a new polar-transformation function from hydraulic flow units. *SPE* 136805
- Thabit GK (1994) Sedimentology of the Nubia group in the area southwest of Aswan, Abu Simbil area. Master's thesis, Assuit University, Egypt, 164 p
- Thorweih U, Heinel M (1993) Groundwater resources and management in SW Egypt: catena supplement. Biomineralization processes of Iron and Manganese. *Berliner geowissenschaftliche Abhandlungen* 26:99–121
- Tiab D, Donaldson EC (1996) *Petrophysics, theory and practice of measuring reservoir rock and fluid transport properties*. Gulf Publ. Co., Houston, Texas, pp 205–220
- Todd DK (1980) *Groundwater hydrology*, 2nd edn. Wiley, New York, p 535p

Publisher's Note Springer Nature remains neutral with regard to jurisdictional claims in published maps and institutional affiliations.